Corral-Ruiz et al. EURASIP Journal on Wireless Communications and Networking (2017) 2017:159
DOI 10.1186/s13638-017-0940-1

EURASIP Journal on Wireless Communications and Networking

RESEARCH Open Access

Modeling and performance analysis for mobile cognitive radio cellular networks

Anum L. Enlil Corral-Ruiz[1], Felipe A. Cruz-Perez[1], S. Lirio Castellanos-Lopez[2*], Genaro Hernandez-Valdez[2] and Mario E. Rivero-Angeles[3]

Abstract

In this paper, teletraffic performance and channel holding time characterization in mobile cognitive radio cellular networks (CRCNs) under fixed-rate traffic with hard-delay constraints are investigated. To this end, a mathematical model to capture the effect of interruption of ongoing calls of secondary users (SUs) due to the arrival of primary users (PUs) is proposed. The proposed model relies on the use of an independent potential interruption time associated with the instant of possible interruption for each ongoing call in every visited cell. Then, a Poisson process is used to approximate the secondary users' call interruption process due to the arrival of PUs. Based on this model and considering that unencumbered service time (UST) and cell dwell time (CDT) of SUs are independent generally distributed random variables, analytical formulae for both the probability distributions of channel holding times and inter-cell handoff attempts rate are derived. Also, a novel approximated closed-form mathematical expression for call forced termination probability of SUs is derived under the restriction that the UST is exponentially distributed. Additionally, by considering all the involved time variables exponentially distributed and employing fractional channel reservation to prioritize intra- and inter-cell handoff call attempts over new call requests, a queuing analysis to evaluate the call-level performance of CRCNs in terms of the maximum Erlang capacity is developed. The accuracy of our proposed mathematical models is extensively investigated under a variety of different evaluation scenarios for all the considered call-level performance metrics. Numerical results demonstrate that channel holding time statistics are highly sensitive to both interruption probability of ongoing secondary calls and type of probability distribution functions used to model CDT and UST. From the teletraffic perspective, numerical results reveal that the system Erlang capacity largely depends on the relative value of the mean secondary service time to the mean primary service time and the primary channels' utilization factor. Also, the obtained results show that there exists a critical utilization factor of the primary resources from which it is no longer possible to guarantee the required quality of service of SUs and, therefore, services with hard-delay constraints cannot be even supported in CRCNs.

Keywords: Cognitive radio cellular networks, Erlang capacity, Call admission control, Cell dwell time, Channel holding time, Call forced termination probability, New call blocking probability, Handoff failure probability, Intra- and inter-cell handoff

1 Introduction

Cognitive radio (CR), which enables secondary users (SUs) to temporarily utilize in an opportunistic fashion the non-in-use spectrum bands allocated to the primary users (PUs) of the spectrum, has been proposed as a promising technology to improve spectrum usage and solving the problem of heterogeneity of radio devices [1]. In Table 1, a list of the acronyms used in the manuscript is provided. In CR networks (CRNs), spectrum handoff allows interrupted secondary calls to be switched to an idle channel, if one is available, to continue its service. Due to the great interest in providing multimedia service with stringent quality of service (QoS) over CR networks [2–5], it is highly desirable for CRNs to support real-time traffic with QoS provisioning. In this research direction, there is a lot of research focused on the QoS provisioning for the secondary sessions; see [2–6] and the references therein.

Recently, implementation of cognitive radio cellular networks (CRCNs) has been investigated to solve both

* Correspondence: salicalo@correo.azc.uam.mx
[2]Electronics Department, UAM, Mexico City, Mexico
Full list of author information is available at the end of the article

Table 1 List of acronyms

Acronyms	Description
CCDF	Complementary cumulative distribution function
CDT	Cell dwell time: the time that a mobile station spends in the jth (for $j = 0, 1,\ldots$) handed off cell irrespective of whether it is engaged in a call or not
CDTr	Residual cell dwell time: the time between the instant that a new call of a user is initiated and the instant that the user is handed off to another cell
CHT	Channel holding time: the amount of time a call holds a channel in a cell
CHTh	Handoff call channel holding time
CHTn	New call channel holding time
CoV	Coefficient of variation
CR	Cognitive radio
CRCN	Cognitive radio cellular networks
FR-HDC	Fixed-rate with hard-delay constraints
IT	Interruption time
LT	Laplace transform
MS	Mobile station
NSH	Without spectrum handoff
PU	Primary user
QoS	Quality of service
RV	Random variable
SH	Spectrum handoff
Sk	Skewness
SU	Secondary user
UCIT	Unencumbered call interruption time: the period of time from the instant a secondary call establish a radio link with a cell until the time it would be interrupted due to the arrival of a PU assuming that the network has unlimited resources and the service time is of infinite duration
UST	Unencumbered service time: the amount of time that the call would remain in progress if it experiences no forced termination
USTr	Residual unencumbered service time: the remaining service time after an ongoing SU has been handed off to another cell

spectrum inefficiency and spectrum scarcity [4, 5]. The main differences between traditional cellular networks and CRCNs lie in the so-called spectrum handoff, interruption due to the arrival of PUs (including the possibility of interruption of multiple sessions of SUs due to non-homogeneous bandwidth of PU and SU channels), and the fluctuating nature of spectrum resource because of the arrival and departure of PUs. In CRCNs, SUs are allowed to perform spectrum handoff within a given CR cell (a.k.a. intra-cell handoff) as well as inter-cell handoff among different CR cells [7]. Developing analytical models for the performance analysis of CRCNs that effectively capture relevant aspects of these complex networks represents a very challenging and important topic of research. This is the topic of research of the present paper. Specifically, teletraffic performance and channel holding time characterization of CRCNs under fixed-rate traffic with stringent-delay constraints are investigated.

Channel holding time (CHT), unencumbered service time (UST), and cell dwell time (CDT) are fundamental time variables to model and analyze the performance of mobile cellular networks. To realistically capture the overall effects of users' mobility and traffic flow characteristics of a real system, the use of general distributions for modeling UST and CDT has been highlighted in previous works [8–12]. These time variables are of primary importance as they can be used to derive other key performance metrics such as new call blocking, handoff failure, and call forced termination probabilities, as well as inter-cell handoff arrival rate and system Erlang capacity. However, none of the previous studies that investigate the functional relationship between CHT, UST, CDT, and their impact on system performance have considered the fluctuating nature of spectrum availability in CRCNs. Moreover, the effect of mobile users across multiple cells has not received enough attention in CRCNs in part because it is a recent topic of research [7, 13, 14]. Thus, service interruption of ongoing secondary sessions due to the arrival of a PU, spectrum handoff, and user mobility must be jointly captured in the teletraffic model for the performance analysis of CRCNs, which represents an important but unexplored topic of research in CR networks to date.

In this paper, the call-level performance analysis of mobile CRCNs under fixed-rate with hard-delay constraints (FR-HDC) traffic[1] is investigated. This issue is addressed in the following manner: (a) as a first step, a novel mathematical model to approximately capture the effect of interruption of SU calls due to the arrival of primary sessions is proposed. In particular, it is proposed to use an independent potential time (referred hereafter as *unencumbered call interruption time*) associated with the instant of possible interruption for each call in every visited cell. (b) Then, the SUs' call interruption process due the arrival of primary users is approximated by a Poisson process.[2] (c) Building on this model and under the assumption that both CDT and UST have general probability distribution functions, analytical formulae for the probability distribution functions and the first three standardized moments of new call channel holding time (CHTn) and handoff call channel holding time (CHTh) as well as mathematical expressions for inter-cell and intra-cell handoff arrival rates are derived. Additionally, for exponentially distributed UST and generally distributed CDT, a novel closed-form mathematical expression for call forced termination probability of SUs (due to

either inter-cell or intra-cell handoff failures) is derived. (d) On the other hand, considering all the involved time variables (i.e., unencumbered call interruption time, unencumbered service time, inter-arrival time, and cell dwell time) exponentially distributed and using fractional channel reservation to prioritize intra (due to spectrum handoff)- and inter (due to users' mobility)-cell handoff call attempts over new call requests, a queuing analysis to evaluate the call-level performance of CRCNs with FR-HDC traffic in terms of Erlang capacity is developed. (Erlang capacity is obtained by optimizing the number of reserved channels.) (e) Finally, channel holding time statistics and the effects of the relative value of the mean secondary service time to the mean primary channel holding time, users' mobility, the use of spectrum handoff (SH), and the primary channel utilization factor on the maximum Erlang capacity of the system are investigated.

Traffic modeling and call-level performance evaluation of wireless cellular communication systems have been widely investigated in the literature [9, 10, 15, 16] (and the references therein). Different performance metrics have been investigated (channel holding time probability distribution, completion probability, forced termination probability, new call blocking probability, among others); however, most published works on traffic modeling in wireless cellular communication systems have considered exponentially distributed UST. Exceptions of this are references [9, 10, 15, 16]. In [9, 15, 16], channel holding times for new and handoff calls are analyzed considering general distributed CDT. In [10], it is additionally considered that the UST is generally distributed.

On the other hand, teletraffic analysis of wireless communication systems taking into account both resource insufficiency and link unreliability is addressed in [9, 17–19]. In [17], Zhang et al. derived mathematical expressions for the probability that a call complete successfully considering the concurrent impacts of the bad quality in the channel and the lack of radio resources. In [18], Zhang studied the impact of Rayleigh fast fading on various teletraffic QoS metrics in wireless networks taking into account carrier frequency. In [19], a closed-form formula for the call completion probability is developed under the generalized wireless channel model and the general CHT distribution using theory of complex variable and transform techniques (Laplace-Stieltjes transform and z-transform). The mathematical models considered in [17–19] are based on link-level statistics.[3]

Contrary to [17–19], in our early work [9], a teletraffic analysis is performed taking into account both resource insufficiency and channel unreliability through a system-level model by introducing a simple call interruption process to model the effect of wireless channel unreliability. Mathematical expressions for the call forced termination probability and inter-cell handoff arrival rate are derived for general distributed CDT and unencumbered call interruption time. Nonetheless, in [9], the UST is assumed to be exponentially distributed.

It is important to notice that none of the described papers so far have considered the particular features of CRNs. In particular, neither call interruption due to the arrival of PUs, intra-cell spectrum handoff, nor the fluctuating nature of spectrum resource was considered. As stated in [7], there has been little investigation so far on the opportunistic spectrum access performance in the presence of inter-cell handoff calls. Most studies have focused considering a single CRN, and therefore, users' mobility and inter-cell handoffs have been neither modeled nor evaluated. In [7], by considering a homogeneous cognitive radio multi-cellular system, both inter-cell handoff rate and forced termination probability of SUs are determined. Reference [20] extends the reported work in [7] by considering that instead of channel reservation, the queueing buffer is used to give both intra-handoff and inter-handoff SU calls priority over the initial SU calls. In [21], the performance of secondary users at the packet level in a cognitive radio cellular network was analyzed, where the transmitter and receiver are not able to communicate directly. In [21], it is considered that packets are delay sensitive and can tolerate a limited amount of waiting time. Additionally, the effect of errors in spectrum sensing on the performance of SUs is addressed in [21]. On the other hand, in [22], multirate cognitive radio cellular networks where the users of each class have a different bandwidth requirement are considered. Two call admission control (CAC) policies are studied, and the system is modeled by considering as a multi-dimensional Markov process. An iterative algorithm to find the steady-state probability distribution and compute the performance measures is proposed. Finally, in our previous related work [23], the impact of mobility of both primary and secondary users on the performance of cognitive radio mobile cellular networks with real-time traffic is investigated. In [23], it is considered that all the involved time variables are modeled by exponentially negative random variables for both secondary and primary calls. However, no closed-form mathematical expressions are obtained and only exponentially distributed CDT and UST are considered in [7, 20–23]. Furthermore, channel holding times are not analyzed, and Erlang capacity is not addressed in [7, 20–23].

In [13, 24], a non-homogeneous cognitive radio network with multiple cells (i.e., cognitive radio base stations) is proposed and analytically evaluated. Probabilities of dropping and blocking for PUs and SUs and forced termination for SUs are investigated. Additionally, a resource planning method to compensate for the

uneven traffic load distribution is proposed in [24]. Due to the non-homogeneous characteristic of the considered network, a pair of variables is needed to represent the state of each cell. To avoid the state space explosion, a small topology of cell is considered. All the involved times are considered exponentially distributed, and no mathematical expression for the considered performance metrics are obtained in [13, 24]. Finally in [14], a spectrum-aware mobility management scheme for CRCNs is proposed. Firstly, a novel CRCN architecture based on the spectrum pooling to mitigate heterogeneous spectrum availability is introduced. Considering spectrum mobility management, user mobility, and inter-cell resource allocation, a unified mobility management framework is developed. Cell capacity, handoff rate, drop rate, and link efficiency are evaluated by simulation. However, neither mathematical modeling nor analysis is presented in [14].

It is important to notice that the mathematical analysis developed in the present paper is based on the analytical framework proposed by Fang in [25, 26] and by Wang and Fan in [10] for the performance evaluation for wireless networks and mobile computing systems. Nevertheless, in [10, 25, 26], particular features of CRNs are not considered and forced call termination is considered to occur due only to resource insufficiency.

The remainder of this paper is structured as follows. In Section 2, the cognitive radio cellular system model is described. Also, in Section 2, the proposed modeling for the call interruption process (due to the arrival of primary users) is introduced. General mathematical expressions for CHT are derived in Section 3, while analytical formulae for inter-handoff rate and forced termination probability are derived in Section 4. In Section 5, a queuing analysis to evaluate the call-level performance of CRCNs in terms of the maximum Erlang capacity is developed. In Section 6, numerical evaluations are carried out for the performance analysis of CRCNs. Finally, Section 7 shows the conclusions.

2 System and proposed call interruption modeling

In this section, the general guidelines for the mathematical analysis of cognitive radio cellular networks under fixed-rate secondary traffic with hard-delay constraints are presented. As stated before, for this type of traffic, it is considered that both blocked and interrupted (due to either inter-cell or intra-cell handoff failures) calls are clear from the system. That is, a secondary type of traffic that has the most stringent QoS requirements (such as the unsolicited grant service class in mobile WiMAX) is considered. Hence, the principal performance metrics are new call blocking, call interruption, and forced call termination probabilities. A homogeneous infrastructure-based mobile CRCN with omni-directional antennas located at the center of each cell is assumed. That is, the structures of all cells within the CRCN are statistically identical. It is assumed that two types of radio users coexist: the licensed (primary) holders of the spectrum and the unlicensed (secondary) users that opportunistically share the spectrum resources with the PUs within the service area of the CRCN, while causing negligible interference to the PUs. PUs are not aware of the existence of SUs' activities, and SUs can detect activities of PUs through spectrum sensing. In this environment, PUs have absolute priority over SUs. The spectrum consists of M primary bands, and each primary band is divided into N sub-bands. Thus, there exist NM sub-bands that are shared by the primary and secondary users. SUs are only allowed to transmit when PUs are not using the spectrum. This resource allocation strategy is shown in Fig. 1. Thus, when an idle primary channel is detected, SUs may temporally occupy this unused channel. If a PU decides to access a primary channel, all SUs using this channel must relinquish their transmission immediately. These unfinished secondary calls are directed to other available channel (this process is called spectrum handoff).[4] If no vacant channels are available, interrupted secondary sessions are dropped. Some other relevant assumptions and definitions are given below. In Table 2, a list of the variables used in the manuscript is provided.

As in [7, 20–22], it is considered that secondary users only use empty channels (resources not being used by primary users) for their data transmission. Since primary users are using a cellular system where co-channel interference is tightly controlled and surveyed in order to guarantee an adequate QoS of cellular users, then co-channel interference is also controlled for the secondary users. In other words, the co-channel interference generated by the secondary users is the same interference generated by the primary users.

Modeling the spectrum sensing error has been widely addressed in the open literature [4, 27–32]. For instance, some previous works advice the use of sensor nodes placed in the serving area to perform this task or even secondary nodes can perform a collaborative sensing by

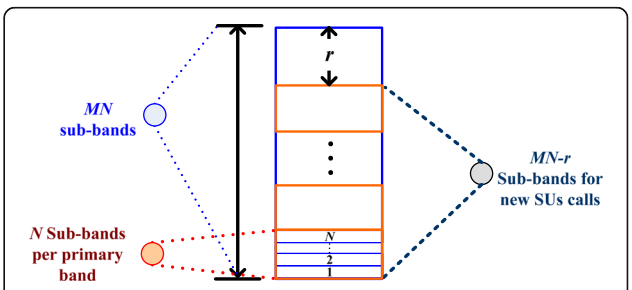

Fig. 1 Block diagram of the resource allocation strategy considered

Table 2 List of variables

Variables	Description
$\lambda^{(P)}$	Arrival rate per cell of PUs' calls
λ_h	Inter-cellular handoff rate
$\lambda_h^{(\text{in})}$	Incoming handoff rate
$\lambda_h^{(\text{out})}$	Outgoing handoff rate
λ_n	Arrival rate per cell of SUs' calls
$f_{X_a^{(P)}}(t)$	Probability density function of the inter-arrival time of PUs' calls
$f_{X_c^{(n)}}(t)$	Probability density function of the CHTn
$f_{X_c^{(h)}}(t)$	Probability density function of the CHTh
$f_{X_{\text{int\_PU}}}(t)$	Probability density function of the unencumbered call interruption time
$f_{X_r}(t)$	Probability density function of the CDTr
$f_X^*(s)$	Laplace transform of the probability density function (pdf) of the random variable X
$F_X^*(s)$	Laplace transform of the cumulative distribution function (CDF) of the random variable X
$f_{X_s}(t)$	Probability density function of the UST
$f_{X_{sr}}(t)$	Probability density function of the USTr
k	The number of active cognitive users that have to relinquish their respective sub-channel due to the arrival of a PU service request
M	Number of primary bands in the system
N	Number of sub-bands which a primary band is divided; N sub-bands are equivalent to one primary band
$N^{(P)}(t)$	It is a RV used to represent the number of PU's arrivals in the interval $[0, t]$.
p	Probability to reserve $\lfloor r \rfloor + 1$ sub-bands
$P(\mathbf{x})$	The state $\mathbf{x}$ stationary probability
$P_b^{(S)}$	The new call blocking probability for SUs
P_{b_tr}	Maximum acceptable values of the new call blocking
P_{ft}	Forced call termination probability
P_{ft_tr}	Maximum acceptable values of the forced call termination
P_{ft}^H	Probability that a SU attempts a handoff procedure as it leaves its current cell and there are no available resources in the target cell
P_{ft}^{Int}	Probability that an interruption occurs due to an arrival of a PU that requires the resources used by the SU
P_{hi}	Probability of intra-cell handoff failure (due to either that an interrupted SU cannot find available resources to perform spectrum handoff or spectrum handoff is not employed)
P_{hl}	Inter-cellular handoff failure probability: the probability that the handoff fails due to the lack of resources as a secondary user moves from one cell to another
P_{Int}	Probability that the analyzed call is interrupted by the first arrival of a PU after the beginning of the call
r	Number of reserved sub-channels to prioritize both intra (due to spectrum handoff)- and inter (due to users' mobility)-cell handoff call attempts over new call requests
x_i	State variable to represent the number of PUs when $i = 0$ and the number of SUs when $i = 1$
$\mathbf{x} = (x_0, x_1)$	Vector of state variables
$x_d^{(j)}$	It is a variable to represent a given/particular value of the CDT in the jth handed off cell
x_r	It is a variable to represent a given/particular value of the CDTr
x_s	It is a variable to represent a given/particular value of the UST
x_{sr}	It is a variable to represent a given/particular value of the USTr
$X_a^{(P)}$	It is a RV used to represent the inter-arrival time of PUs calls
$X_c^{(n)}$	It is a RV used to represent the CHTn of secondary users
$X_c^{(h)}$	It is a RV used to represent the CHTh of secondary users
$X_d^{(j)}$	It is a RV used to represent the CDT of secondary users in the jth handed off cell
X_{int_PU}	It is a RV used to represent the unencumbered call interruption time
X_r	It is a RV used to represent the CDTr of secondary users
X_s	It is a RV used to represent the UST of secondary users
X_{sr}	It is a RV used to represent the USTr of secondary users
$1/\mu$	$E\{X_s\} = 1/\mu$ is the mean value of X_s (UST of secondary users)
$1/\mu^{(P)}$	Mean value of UST of primary users

sharing their own information regarding the status of the channel in order to make a more accurate decision. Note that these alternatives are open issues and we believe that lay outside the scope of this work. In the submitted manuscript, it is considered that ongoing secondary users can sense the activity of primary users instantaneously and reliable (i.e., ideal spectrum sensing is assumed). In this sense, the obtained performance metrics can be considered as an upper bound [33]. It has been shown in the literature [4, 27–30] that the effect of false alarm and misdetection can be plugged with no major problem into most of the developed mathematical analysis of cognitive radio networks (CRNs). However, in this paper, to keep our mathematical analysis simple and to concentrate our study into the pure performance of the cognitive cellular radio network, we assume ideal spectrum sensing (spectrum sensing is error free). This

represents a reasonable assumption in CRNs where a sensor network having enough sensors performing collaborative sensing of the radio environment in space and time is employed, as it is considered in [34, 35]. Modeling spectrum sensing error in CRNs has been addressed in [4, 27–30]. Additionally, the effect of unreliable spectrum sensing in CRNs under voice over Internet Protocol traffic is investigated in our early work [4]. Also as in [4], it is assumed that service events are unlikely to happen during the sensing period since the sensing periods are relatively small. Several works has evaluated (quantitatively and qualitatively) the extent by which spectrum sensing errors affect the performance of CRNs [4, 27–30].

First, the UST per call of SUs x_s is the amount of time that the call would remain in progress if it experiences no forced termination. Unless otherwise specified, this quantity is modeled by a generally distributed random variable (RV). The RV used to represent this time is X_s, and its mean value is $E\{X_s\} = 1/\mu$. The pdf of the UST is represented by $f_{X_s}(t)$. On the other hand, the mean UST of PUs is $1/\mu^{(P)}$.

The residual unencumbered service time (USTr) x_{sr} is defined as the remaining service time after an ongoing SU has been handed off to another cell. The RV used to represent residual UST is X_{sr}. The pdf of the USTr is represented by $f_{X_{sr}}(t)$, and it is derived in Section 3.2.

Now, CDT $x_d^{(j)}$ is defined as the time that a mobile station (MS) spends in the jth (for $j = 0, 1,\ldots$) handed off cell irrespective of whether it is engaged in a call or not. The RVs used to represent these times are $X_d^{(j)}$ (for $j = 0, 1,\ldots$) and are assumed to be independent and generally distributed. For homogeneous cellular systems, this assumption has been widely accepted in the literature [10].

The residual CDT (CDTr) x_r is defined as the time between the instant that a new call of a user is initiated and the instant that the user is handed off to another cell. Notice that always $x_d^{(0)} > x_r$ because the beginning of residual cell dwell time is randomly chosen within a cell dwell time interval. The RV used to represent CDTr is X_r. Thus, the pdf of the CDTr, $f_{X_r}(t)$, can be calculated in terms of the cell dwell time using the well-known residual life theorem [9] as follows:

$$f_{X_r}(t) = \frac{1 - F_{X_d}(t)}{E\{X_d\}} \tag{1}$$

and its corresponding Laplace transform is given by

$$f^*_{X_r}(s) = \frac{\left[1 - f^*_{X_d}(s)\right]}{E\{X_d\}s} \tag{2}$$

CHT is defined as the amount of time a call holds a channel in a cell. Let $X_{c^{(n)}}$ and $X_{c^{(h)}}$ denote, respectively, the CHTn and the CHTh with their corresponding pdfs $f_{X_c^{(n)}}(t)$ and $f_{X_c^{(h)}}(t)$. The relationship between the above defined times is illustrated in Fig. 2.

Call arrivals of PUs and SUs are assumed to follow independent Poisson processes with mean arrival rate $\lambda^{(P)}$ and λ_n arrivals per second per cell, respectively. Since the arrival process for the PUs follows a Poisson process, then the pdf of the inter-arrival time of PUs $X_a^{(P)}$ is given by $f_{X_a^{(P)}}(t) = \lambda^{(P)} e^{-\lambda^{(P)} t}$.

2.1 Proposed model for the call interruption time

In this sub-section, a simple but fundamental mathematical model to capture the effect of interruption of SU's calls due to the arrival of primary users is proposed. The proposed model relies on the use of an independent potential interruption time (referred as unencumbered call interruption time and it is denoted by $X_{\text{int\_PU}}$, with pdf $f_{X_{\text{int\_PU}}}(t)$) associated with the instant of possible interruption for each ongoing call in every visited cell. The relationship between this time and the rest of the times is illustrated in Fig. 3.

The unencumbered call interruption time is defined as the period of time from the instant a secondary call establish a radio link with a cell until the time it would be interrupted due to the arrival of a PU assuming that the network has unlimited resources and the service time is of infinite duration. Physically, this time represents the period of time that a secondary call last before it would be abruptly terminated due to a primary call arrival under the assumption that both the cell dwell time and the unencumbered service time are of infinite duration. The call interruption time is said to be "unencumbered" because the interruption of a secondary call in progress by a primary user arrival can or cannot occur, depending on the values of the CDT and the UST. Thus, a particular secondary call is interrupted in the current cell if and only if its potential call interruption time is smaller than both the unencumbered service time and residual cell dwell time (or both the unencumbered residual service time and cell dwell time). Therefore, notice that this call interruption time is not a measurable physical quantity. Indeed, in case that the user leaves the cell or completes its call before the call is interrupted, it is not possible to know the actual value of this interruption time since, in this case, call interruption due to the arrival of primary users actually never happens.

The probability distribution probability of the unencumbered call interruption time (IT) is related to the arrival process of PUs and the stochastic processes of the numbers of PUs and SUs with ongoing calls. In this work, in order to obtain a tractable mathematical analysis, it is proposed to approximate the secondary users' call interruption process due the arrival of primary users by a Poisson one. This proposed model is detailed next.

As stated above, the IT of an analyzed SU call due to an arrival of a PU is the elapsed time from the beginning

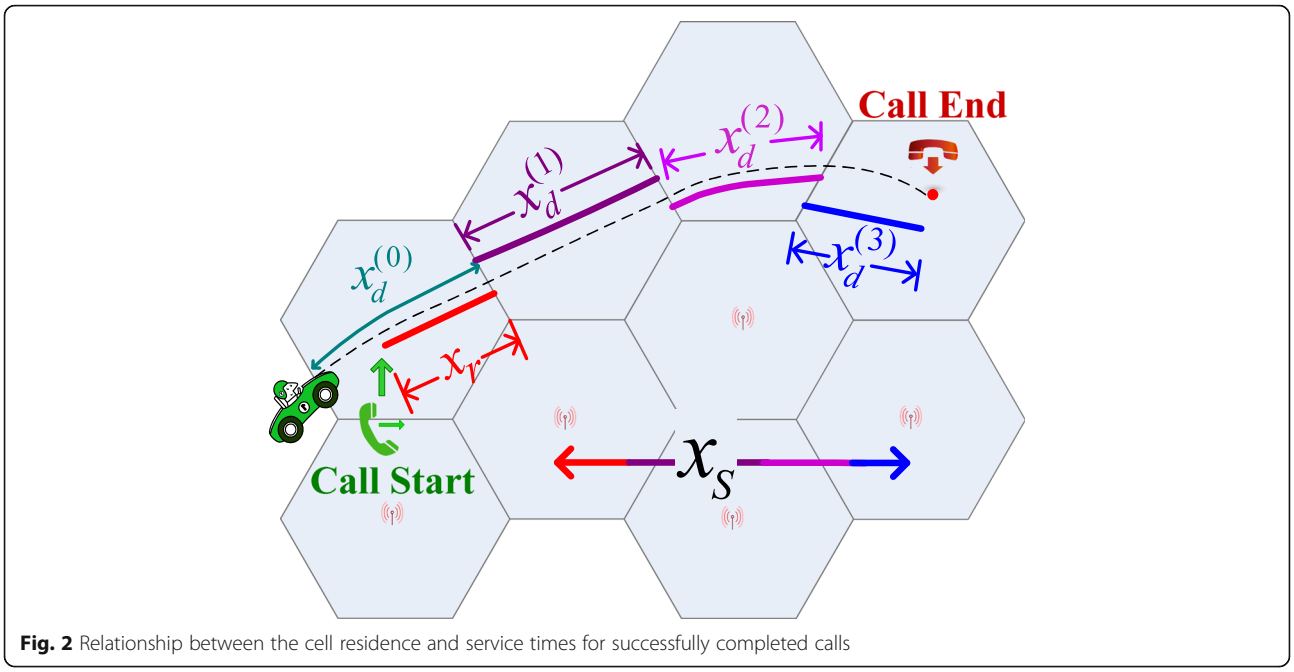

Fig. 2 Relationship between the cell residence and service times for successfully completed calls

of the call until the arrival of a PU that causes the interruption of the call. Building on this, let us define P_{Int} as the probability that an arrival of a PU interrupts the analyzed call.[5] As an approximation and for the sake of mathematical tractability, it is considered that the interruption probability is independent for each individual user.[6] As shown below, with this approximation, the call interruption process of SUs due the arrival of PUs is a Poisson process. However, as it is shown in Appendix 1, the call interruption process of SUs due the arrival of PUs does not actually follow a Poisson one. In Section 6, the inaccuracy introduced by this approximation in the numerical results is extensively investigated under a variety of different evaluation scenarios for all the considered call-level performance metrics.

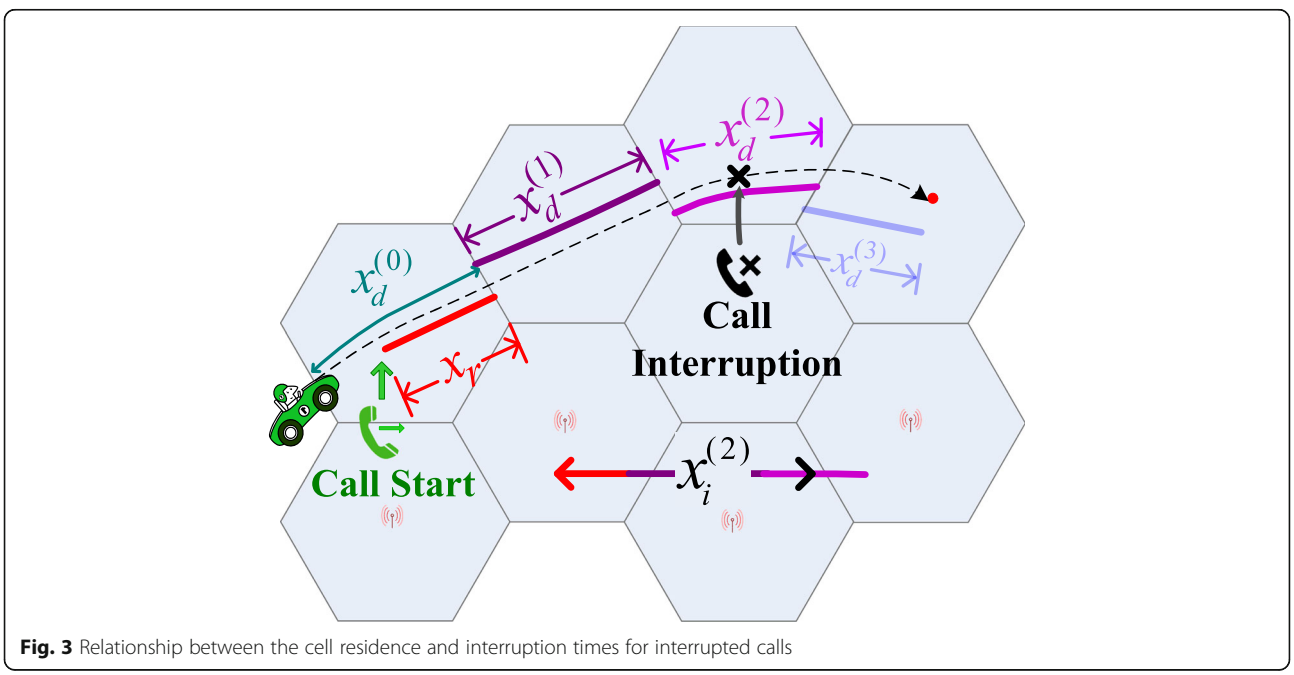

Fig. 3 Relationship between the cell residence and interruption times for interrupted calls

Due to the memory-less property of the exponential distribution of the primary call inter-arrival time, for the case when the analyzed call is interrupted by the first arrival of a PU after the beginning of the call (which occurs with probability P_{Int}), the elapsed time until the interruption is $X_{a(1)}{}^{(P)}$. In the case when the analyzed SU call is interrupted by the arrival of the second PU after the beginning of the SU call, the elapsed time is $X_{a(1)}{}^{(P)} + X_{a(2)}{}^{(P)}$ and occurs with probability $(1 - P_{\text{Int}})$ P_{Int}, and so on and so forth. Then, the pdf of $X_{\text{int\_PU}}$ is given by

$$\begin{aligned} f_{X_{\text{int\_PU}}}(t) &= P_{\text{Int}} \sum_{i=0}^{\infty} (1-P_{\text{Int}})^i f_{\sum_{j=1}^{i+1} X_{a(j)}^{(P)}} \\ (t) &= P_{\text{Int}} \sum_{i=0}^{\infty} (1-P_{\text{Int}})^i \frac{\left(\lambda^{(P)}\right)^{i+1} t^i}{i!} e^{-\lambda^{(P)} t} \\ &= P_{\text{Int}} \lambda^{(P)} e^{-P_{\text{Int}} \lambda^{(P)} t} \end{aligned} \tag{3}$$

From (3), it is clear that the elapsed time from the beginning of the secondary call until it is interrupted due to the arrival of a primary call is exponentially distributed with mean $\mathrm{E}\{X_{\text{int\_PU}}\} = 1/(P_{\text{Int}}\lambda^{(P)})$.

In this paper, the pdf, the cumulative distribution, and the Laplace transform (LT) of a given RV, say X, are denoted by $f_X(t)$, $F_X(t)$, and $f_X^*(s)$, respectively. It is assumed that $f_X^*(s)$ is a rational function in the analysis developed in Sections 3 and 4. In the following analysis, we focus on the performance of secondary users.

3 Channel holding time statistics

In this section, the probability distributions of the CHTn and CHTh in CRCNs are derived for general distributions of both unencumbered service time and cell dwell times.

3.1 New call channel holding time

In this section, the pdf of the CHTn is derived. To this end, notice that SUs that access the system release their assigned resources in the same cell that they were assigned for the following reasons: (a) the SU completes its service (in this case, the new call channel holding time equals the service time, X_s); (b) the SU leaves the cell where it arrived (in this case, the new call channel holding time equals the residual cell dwell time, X_r); or (c) the SU's call is interrupted due to a primary arrival (in this case, the CHTn equals $X_{\text{int\_PU}}$). As such, the CHTn can be expressed as follows:

$$X_c^{(n)} = \min\left(X_s,\ X_r, X_{\text{int\_PU}}\right) \tag{4}$$

Considering (3), the Laplace transform of the CDF is given by

$$\begin{aligned} F^*_{X_c^{(n)}}(s) = &\frac{f^*_{X_s}(s)}{s} + \frac{f^*_{X_r}(s)}{s} + \frac{f^*_{X_{\text{int\_PU}}}(s)}{s} \\ &- \int_0^{\infty} F_{X_{\text{int\_PU}}}(t)\ F_{X_s}(t)\ e^{-st} dt \\ &- \int_0^{\infty} F_{X_{\text{int\_PU}}}(t)\ F_{X_r}(t)\ e^{-st} dt \\ &- \int_0^{\infty} F_{X_s}\ (t)\ F_{X_r}\ (t)\ e^{-P_{\text{Int}}\lambda^{(P)}t} e^{-st} dt \end{aligned} \tag{5}$$

In [10], it is shown that

$$\begin{aligned} \int_0^{\infty} F_X(t)\ F_Y(t)\ e^{-st} dt = &\frac{f^*_Y(s)}{s} \\ &- \sum_{p \in \Omega_X} \underset{\xi = s+p}{\mathbf{Res}} \frac{f^*_Y(\xi)}{\xi}\ \frac{f^*_X(s-\xi)}{s-\xi} \end{aligned} \tag{6}$$

where Ω_X is the set of poles of $f^*(-s)$ and $\underset{\xi=s+p}{\mathbf{Res}}$ denotes the residue at pole $\xi = s + p$. Hence, substituting (6) in (5) and simplifying,

$$\begin{aligned} F^*_{X_c^{(n)}}(s) = &\frac{f^*_{X_{\text{int\_PU}}}(s)}{s} \\ &+ \sum_{p \in \Omega_{X_{\text{int\_PU}}}} \underset{\xi = s+p}{\mathbf{Res}} \frac{f^*_{X_s}(\xi)}{\xi} \frac{f^*_{X_{\text{int\_PU}}}(s-\xi)}{s-\xi} \\ &+ \sum_{p \in \Omega_{X_{\text{int\_PU}}}} \underset{\xi = s+p}{\mathbf{Res}} \frac{f^*_{X_r}(\xi)}{\xi} \frac{f^*_{X_{\text{int\_PU}}}(s-\xi)}{s-\xi} \\ &- \int_0^{\infty} F_{X_s}(t) F_{X_r}(t) e^{-P_{\text{Int}}\lambda^{(P)}} t e^{-st} dt \end{aligned} \tag{7}$$

Since $f^*_{X_s}(0) = 1$, the last part of (7) can be expressed as

$$\begin{aligned} - \int_0^{\infty} F_{X_s}(t) F_{X_r}(t) e^{-P_{\text{Int}}\lambda^{(P)}} t e^{-st} dt = &- \frac{f^*_{X_r}\left(s + P_{\text{Int}}\lambda^{(P)}\right)}{s + P_{\text{Int}}\lambda^{(P)}} \\ + \sum_{p \in \{\Omega_{X_s}\}} &\underset{\xi = s + P_{\text{Int}}\lambda^{(P)} + p}{\mathbf{Res}} \frac{f^*_{X_r}(\xi)}{\xi} \frac{f^*_{X_s}\left(s + P_{\text{Int}}\lambda^{(P)} - \xi\right)}{s + P_{\text{Int}}\lambda^{(P)} - \xi} \end{aligned} \tag{8}$$

Substituting (8) in (7) we obtain

$$F^*_{X_{c(n)}}(s) = \frac{f^*_{X_{\text{int\_PU}}}(s)}{s} + \sum_{p\in\Omega_{X_{\text{int\_PU}}}} \mathbf{Res}_{\xi=s+p} \frac{f^*_{X_s}(\xi)}{\xi}\frac{f^*_{X_{\text{int\_PU}}}(s-\xi)}{s-\xi} + \sum_{p\in\Omega_{X_{\text{int\_PU}}}} \mathbf{Res}_{\xi=s+p} \frac{f^*_{X_r}(\xi)}{\xi}\frac{f^*_{X_{\text{int\_PU}}}(s-\xi)}{s-\xi}\frac{f^*_{X_r}\left(s+P_{\text{Int}}\lambda^{(P)}\right)}{s+P_{\text{Int}}\lambda^{(P)}} + \sum_{p\in\{\Omega_{X_s}\}} \mathbf{Res}_{\xi=s+P_{\text{Int}}\lambda^{(P)}+p} \frac{f^*_{X_r}(\xi)}{\xi}\frac{f^*_{X_s}\left(s+P_{\text{Int}}\lambda^{(P)}-\xi\right)}{s+P_{\text{Int}}\lambda^{(P)}-\xi} \tag{9}$$

Considering the Laplace Transform of the pdf of $X_{\text{Int\_PU}}$, shown in Appendix 2, (9) can be written as

$$F^*_{X^{(n)}_c}(s) = \frac{f^*_{X_{\text{int\_PU}}}(s)}{s} - \frac{f^*_{X_r}\left(s+P_{\text{Int}}\lambda^{(P)}\right)}{s+P_{\text{Int}}\lambda^{(P)}} + \lim_{\xi\to s+\lambda^{(P)}P_{\text{Int}}} \left(\xi-s-\lambda^{(P)}P_{\text{Int}}\right)\frac{f^*_{Xs}(\xi)}{\xi}\frac{\lambda^{(P)}P_{\text{Int}}}{(s-\xi)\left(\lambda^{(P)}P_{\text{Int}}+s-\xi\right)} + \lim_{\xi\to s+\lambda^{(P)}P_{\text{Int}}} \left(\xi-s-\lambda^{(P)}P_{\text{Int}}\right)\frac{f^*_{X_r}(\xi)}{\xi}\frac{\lambda^{(P)}P_{\text{Int}}}{(s-\xi)\left(\lambda^{(P)}P_{\text{Int}}+s-\xi\right)} + \sum_{p\in\{\Omega_{X_s}\}} \mathbf{Res}_{\xi=s+P_{\text{Int}}\lambda^{(P)}+P} \frac{f^*_{X_r}(\xi)}{\xi}\frac{f^*_{X_s}\left(s+P_{\text{Int}}\lambda^{(P)}-\xi\right)}{s+P_{\text{Int}}\lambda^{(P)}-\xi} \tag{10}$$

After some algebraic manipulation and simplifying,

$$F^*_{X^{(n)}_c}(s) = \frac{\lambda^{(P)}P_{\text{Int}}}{s\left(\lambda^{(P)}P_{\text{Int}}+s\right)} + \frac{f^*_{X_s}\left(s+\lambda^{(P)}P_{\text{Int}}\right)}{s+\lambda^{(P)}P_{\text{Int}}} + \sum_{p\in\{\Omega_{X_s}\}} \mathbf{Res}_{\xi=s+P_{\text{Int}}\lambda^{(P)}+p} \frac{f^*_{X_r}(\xi)}{\xi}\frac{f^*_{X_s}\left(s+P_{\text{Int}}\lambda^{(P)}-\xi\right)}{s+P_{\text{Int}}\lambda^{(P)}-\xi} \tag{11}$$

The Laplace transform of the pdf of CHTn is given by

$$f_{X^{(n)}_c}{}^*(s) = \frac{\lambda^{(P)}P_{\text{Int}}}{\left(\lambda^{(P)}P_{\text{Int}}+s\right)} + \frac{sf^*_{X_s}\left(s+\lambda^{(P)}P_{\text{Int}}\right)}{s+\lambda^{(P)}P_{\text{Int}}} + s\sum_{p\in\{\Omega_{X_s}\}} \mathbf{Res}_{\xi=s+P_{\text{Int}}\lambda^{(P)}+p} \frac{f^*_{X_r}(\xi)}{\xi}\frac{f^*_{X_s}\left(s+P_{\text{Int}}\lambda^{(P)}-\xi\right)}{s+P_{\text{Int}}\lambda^{(P)}-\xi} \tag{12}$$

3.2 Handoff call channel holding time

In this section, the pdf of the CHTh is derived. In the following analysis, we consider that the inter-cellular handoff failure probability P_{hI} (defined as the probability that the handoff fails due to the lack of resources as a secondary user moves from one cell to another) is known. However, this probability is studied in detail in Section 5. To derive the CHTh, notice that an ongoing SUs is successfully handed off to a new cell and the system releases the radio resources assigned in the new cell for the following reasons: (a) the SU completes its service (in this case, the handoff call channel holding time equals the residual service time, X_{sr}); (b) the SU leaves the current cell (in this case, the CHTh equals the cell dwell time, X_d); or (c) the SU's call is interrupted due to a PU arrival (in this case, the CHTh equals $X_{\text{int\_PU}}$). As such, the CHTh can be expressed as follows:

$$X^{(h)}_C = \min\left(X_{sr}, X_d, X_{\text{int\_PU}}\right) \tag{13}$$

Thus, we need to derive the pdf of the USTr. To this end, let us define Y_m as the elapsed time from the beginning of the call to the mth handoff performed for the mobile of interest, then $Y_m = X_r + X_{d(1)} + X_{d(2)} + \ldots + X_{d(m-1)}$ with its Laplace transform given by

$$f^*_{Y_m}(s) = f^*_{X_r}(s)\left[f^*_{X_d}(s)\right]^{m-1} \tag{14}$$

where we have used the fact that $X_{d(i)}$ for i = 1, 2,..., m − 1 are considered independent and identically distributed (*i.i.d.*) RVs. Now, let us denote by $N^{(P)}(t)$ the RV that represents the number of PU's arrivals in the interval [0, t]. Also, let us define the following events: $\{B_m\}$ is the event that the secondary call has experienced m successful handoffs before entering the current cell and {No Int by PU until Y_m} is the event that the call of interest has not been interrupted by PUs until time Y_m. Then,

$$P\{B_m\}-(1-P_{hI})^m P\{X_s > Y_m\}P\{\text{No Int by PU until } Y_m\} \tag{15}$$

Considering a given value for Y_m, say $Y_m = y_m$, the probability of k arrivals in the interval [0,y_m] is

$$P\left\{N^{(P)}(y_m) = k | Y_m = y_m\right\} = \frac{\left(\lambda^{(P)}y_m\right)^k}{k!}e^{-\lambda^{(P)}y_m} \tag{16}$$

and the probability that none of these PU's arrivals interrupts the ongoing SU call is given by $(1 - P_{\text{Int}})^k$. Thus, the probability that the ongoing SU call of interest is not interrupted by the arrivals of PUs until time y_m is given by

$$P\{\text{No Int by PU until } Y_m | Y_m = y_m\} = \sum_{k=0}^{\infty}(1-P_{\text{Int}})^k \frac{\left(\lambda^{(P)}y_m\right)^k}{k!}e^{-\lambda^{(P)}y_m} = e^{-\lambda^{(P)}P_{\text{Int}}y_m} \tag{17}$$

According to the total probability formula, we have

$$P\{\text{No Int by PU until } Y_m\} = \int_0^\infty e^{-P_{\text{Int}}\lambda^{(P)}y_m} f_{Y_m}(y_m)dy_m \tag{18}$$

Using (18) in (15), we have

$$P\{B_m\} = (1-P_{hI})^m P\{X_s > Y_m\} \int_0^\infty e^{-P_{\text{Int}^\lambda}(P)t} f_{Y_m}(t)dt \tag{19}$$

Applying the Laplace transform and then the inverse Laplace transform to the last part of (19)

$$\begin{aligned} P\{B_m\} &= (1-P_{hI})^m P\{X_s > Y_m\} \\ &\times \int_{t=0}^\infty \frac{1}{2\pi j} \int_{\phi=-\infty}^\infty e^{\phi t} f^*_{X_r} \\ &\times \left(\phi + P_{\text{Int}}\lambda^{(P)}\right) \left[f^*_{X_d}\left(\phi + P_{\text{Int}}\lambda^{(P)}\right)\right]^{m-1} d\phi dt \end{aligned} \tag{20}$$

Since

$$\begin{aligned} \int_{t=0}^\infty e^{-P_{\text{Int}}\lambda^{(P)}t} f_{Y_m}(t)dt &= \int_{t=0}^\infty L^{-1}\left\{f^*_{X_r}\left(\phi + P_{\text{Int}}\lambda^{(P)}\right)\right. \\ &\left. \times \left[f^*_{X_d}\left(\phi + P_{\text{Int}}\lambda^{(P)}\right)\right]^{m-1}\right\} dt \end{aligned} \tag{21}$$

where $L^{-1}\{\cdot\}$ represents the inverse Laplace transform whose independent variable is ϕ. From [10],

$$P(X > Y) = -\sum_{p\in\Omega_Y} \mathbf{Res}_{s=p} \frac{f^*_Y(s)}{s} f^*_X(-s) \tag{22}$$

Using the proposition (22) in (20), we have

$$\begin{aligned} P\{B_m\} &= -(1-P_{hI})^m \sum_{p\in\Omega_{X_s}} \mathbf{Res}_{\zeta=p} \frac{f^*_{Y_m}(\zeta)}{\zeta} f^*_{X_s}(-\zeta) \\ &\int_{t=0}^\infty \frac{1}{2\pi j} \int_{\phi=-\infty}^\infty e^{\phi t} f^*_{X_r}\left(\phi + P_{\text{Int}}\lambda^{(P)}\right) \\ &\times \left[f^*_{X_d}\left(\phi + P_{\text{Int}}\lambda^{(P)}\right)\right]^{m-1} d\phi dt \end{aligned} \tag{23}$$

Defining $\Delta = \sum_{m=1}^\infty P\{B_m\}$, it is calculated as

$$\begin{aligned} \Delta = -\sum_{m=1}^\infty \left\{ (1-P_{hI})^m \sum_{p\in\Omega_{X_s}} \mathbf{Res}_{\zeta=p} \frac{f^*_{X_r}(\zeta)\left[f^*_{X_d}(\zeta)\right]^{m-1}}{\zeta} f^*_{X_s}(-\zeta) \int_{t=0}^\infty \frac{1}{2\pi j} \right. \\ \left. \int_{\phi=-\infty}^\infty e^{\phi t} f^*_{X_r}\left(\phi + P_{\text{Int}}\lambda^{(P)}\right) \left[f^*_{X_d}\left(\phi + P_{\text{Int}}\lambda^{(P)}\right)\right]^{m-1} d\phi dt \right\} \end{aligned} \tag{24}$$

Interchanging the order of the summations and integrals, and simplifying, we have

$$\begin{aligned} \Delta &= 1-(1-P_{hI}) \sum_{p\in\Omega_{X_s}} \mathbf{Res}_{s=p} \frac{f^*_{X_r}(\zeta) f^*_{X_s}(-\zeta)}{\zeta} \\ &\int_{t=0}^\infty L^{-1}\left\{ \frac{f^*_{X_r}\left(\phi + P_{\text{Int}}\lambda^{(P)}\right)}{1-(1-P_{hI}) f^*_{X_d}(\zeta) f^*_{X_d}\left(\phi + P_{\text{Int}}\lambda^{(P)}\right)} \right\} dt \end{aligned} \tag{25}$$

Note that the last term in (25) is a constant. Now, notice that the complementary cumulative distribution function (CCDF) of the USTr of the accepted calls can be expressed as

$$1-F_{X_{sr}}(t) = \frac{1}{\Delta} \sum_{m=1}^\infty P\{X_{sr} > t,\ B_m\} \tag{26}$$

Using (19) in (26), we have

$$\begin{aligned} 1-F_{X_{sr}}(t) &= \frac{1}{\Delta} \sum_{m=1}^\infty (1-P_{hI})^m \int_{y=0}^\infty e^{-P_{Int}\lambda^{(P)}y} f_{Y_m}(y)dy \\ &\int_{x=0}^\infty [1-F_{X_s}(t+x)] f_{Y_m}(x)dx \end{aligned} \tag{27}$$

Then, the pdf of the residual unencumbered service time is given by

$$\begin{aligned} f_{X_{sr}}(t) &= \frac{1}{\Delta} \sum_{m=1}^\infty (1-P_{hI})^m \int_{y=0}^\infty e^{-P_{Int}\lambda^{(P)}y} f_{Y_m}(y)dy \\ &\int_{x=0}^\infty f_{X_s}(t+x) f_{Y_m}(x)dx \end{aligned} \tag{28}$$

and its corresponding Laplace transform is given by

$$\begin{aligned} f^*_{X_{sr}}(s) &= \frac{1}{\Delta} \sum_{m=1}^\infty (1-P_{hI})^m \int_{y=0}^\infty e^{-P_{\text{Int}}\lambda(P)y} f_{Y_m}(y)dy \\ &\int_{t=0}^\infty e^{-st} \int_{x=0}^\infty f_{X_s}(t+x) f_{Y_m}(x)dxdt \end{aligned} \tag{29}$$

In [10], it was demonstrated that

$$\begin{aligned} &\int_{t=0}^\infty \int_{x=0}^\infty f_{X_s}(t+x) f_{Y_m}(x) e^{-st} dxdt \\ &= -\sum_{p\in\Omega_{X_s}} \mathbf{Res}_{z=p} \frac{f^*_{Y_m}(z)}{s+z} f^*_{X_s}(-z) \end{aligned} \tag{30}$$

Using (30) in (29), interchanging the orders of the summations and integrals, and simplifying,

$$f^*_{X_{sr}}(s) = -\frac{1}{\Delta}\sum_{p\in\Omega_{X_s}} \mathbf{Res}_{z=p} \frac{f^*_{X_s}(-z)}{s+z} \sum_{m=1}^{\infty} f^*_{Y_m}(z)(1-P_{hI})^m \int_{y=0}^{\infty} e^{-P_{\text{Int}}\lambda^{(P)}y} f_{Y_m}(y)dy \tag{31}$$

Using (21) in (31), we have

$$\begin{aligned} f^*_{X_{sr}}(s) &= -\frac{1}{\Delta}\sum_{p\in\Omega_{X_s}} \mathbf{Res}_{z=p} \frac{f^*_{X_s}(-z)}{s+z} \\ &\quad \times \sum_{m=1}^{\infty} f^*_{Y_m}(z)(1-P_{hI})^m \int_{t=0}^{\infty} L^{-1}\left\{ f^*_{X_r}\left(\xi + P_{\text{Int}}\lambda^{(P)}\right) \right. \\ &\quad \left. \times \left[f^*_{X_d}\left(\xi + P_{\text{Int}}\lambda^{(P)}\right)\right]^{m-1} \right\} dt \\ &= -\frac{(1-P_{hI})}{\Delta}\sum_{p\in\Omega_{X_s}} \mathbf{Res}_{z=p} \frac{f^*_{X_s}(-z)}{s+z} f^*_{X_r}(z) \\ &\quad \times \int_{t=0}^{\infty} L^{-1}\left\{ \frac{f^*_{X_r}\left(\xi + P_{\text{Int}}\lambda^{(p)}\right)}{1-(1-P_{hI})f^*_{X_d}(z) f^*_{X_d}\left(\xi + P_{\text{Int}}\lambda^{(P)}\right)} \right\} dt \end{aligned} \tag{32}$$

Using (25) in (32), we have

$$f^*_{X_{sr}}(s) = -\frac{(1-P_{hI})\sum_{p\in\Omega_{X_s}} \mathbf{Res}_{z=p} \frac{f^*_{X_s}(-z)}{s+z} f^*_{X_r}(z)\delta}{-(1-P_{hI})\sum_{p\in\Omega_{X_s}} \mathbf{Res}_{z=p} \frac{f^*_{X_r}(\zeta) f^*_{X_s}(-\zeta)}{\zeta}\gamma} \tag{33}$$

where $\delta = \int_{t=0}^{\infty} L^{-1}\left\{ \frac{f^*_{X_r}\left(\xi + P_{\text{Int}}\lambda^{(P)}\right)}{\left(s+P_{\text{Int}}\lambda^{(P)}\right)\left[1-(1-P_{hI})f^*_{X_d}(z) f^*_{X_d}\left(\xi+P_{\text{Int}}\lambda^{(P)}\right)\right]} \right\} dt; \gamma = \int_{t=0}^{\infty} L^{-1}\left\{ \frac{f^*_{X_r}\left(\phi+P_{\text{Int}}\lambda^{(P)}\right)}{\left(s+P_{\text{Int}}\lambda^{(P)}\right)\left[1-(1-P_{hI})f^*_{X_d}(\varsigma) f^*_{X_d}\left(\phi+P_{\text{Int}}\lambda^{(P)}\right)\right]} \right\} dt.$

Now, we have all the elements to derive the pdf of the handoff call channel holding time. Thus, using (5), (13), and (33) and following a similar procedure as the one used in Section 3.1 for deriving the LT of the CHTn, the LT of the pdf of the CHTh is found as

$$\begin{aligned} f^*_{X_c^{(h)}}(s) &= \frac{\lambda^{(P)}P_{\text{Int}}}{\left(\lambda^{(P)}P_{\text{Int}} + s\right)} + \frac{s f^*_{X_{sr}}\left(s+\lambda^{(P)}P_{\text{Int}}\right)}{s+\lambda^{(P)}P_{\text{Int}}} \\ &\quad + s\sum_{p\in\{\Omega_{X_{sr}}\}} \mathbf{Res}_{\xi=s+P_{\text{Int}}\lambda^{(P)}+p} \frac{f^*_{X_d}(\xi)}{\xi} \frac{f^*_{X_{sr}}\left(s+P_{\text{Int}}\lambda^{(P)}-\xi\right)}{s+P_{\text{Int}}\lambda^{(P)}-\xi} \end{aligned} \tag{34}$$

An equivalent expression is found using the poles of the CDT. This expression is given by

$$\begin{aligned} f^*_{X_c^{(h)}}(s) &= \frac{\lambda^{(P)}P_{\text{Int}}}{\left(\lambda^{(P)}P_{\text{Int}} + s\right)} + \frac{s f^*_{X_d}\left(s+\lambda^{(P)}P_{\text{Int}}\right)}{s+\lambda^{(P)}P_{\text{Int}}} \\ &\quad + s\sum_{p\in\Omega_{X_d}} \mathbf{Res}_{\xi=s+P_{\text{Int}}\lambda^{(P)}+p} \frac{f^*_{X_{sr}}(\xi)}{\xi} \frac{f^*_{X_d}\left(s+P_{\text{Int}}\lambda^{(P)}-\xi\right)}{s+P_{\text{Int}}\lambda^{(P)}-\xi} \end{aligned} \tag{35}$$

From (12) and (35), it is straightforward to obtain the lth moment of both CHTn and CHTh by obtaining the lth derivative of $f^*_{X_c^{(n)}}(-s)$ and $f^*_{X_c^{(h)}}(-s)$ at $s = 0$, respectively.

4 Forced call termination and inter-cellular handoff arrival rate

In this section, the expressions of both the inter-cell handoff arrival rate and forced termination probability of secondary users are derived.

4.1 Inter-cellular handoff rate for secondary users

For the analysis in this sub-section, both the UST and CDT are considered to be generally distributed. First, the outgoing handoff rate $\lambda_h^{(\text{out})}$ of a given cell can be expressed as follows:

$$\begin{aligned} \lambda_h^{(\text{out})} &= \lambda_n\left(1-P_b^{(s)}\right)P\left\{X_r < \min\left(X_{\text{int\_PU}}, X_s\right)\right\} \\ &\quad + \lambda_h^{(\text{in})}(1-P_{hI})P\left\{X_d < \min\left(X_{\text{int\_PU}}, X_{sr}\right)\right\} \end{aligned} \tag{36}$$

where $P_b^{(S)}$ is the new call blocking probability for SUs and it is considered to be known. This probability is studied in detail in Section 5.

The rationale behind (36) is that in order to have an outgoing inter-cellular handoff for SUs, first, a new call of a SU must arrive and not to be blocked, then it has to leave the cell before its service be either interrupted by the arrival of a PU or successfully completed. Also, incoming calls from other cells (with rate $\lambda_{h^{(\text{in})}}$) must be accepted (a successful handoff) and the users with those calls have to leave the cell before their respective (residual) services be either interrupted by the arrival of a PU or completed. In a homogenous system in steady state, the following condition must be hold $\lambda_h = \lambda_h^{(\text{out})} = \lambda_h^{(\text{in})}$. Then, from (36), we get

$$\lambda_h = \frac{\lambda_n\left(1-P_b^{(s)}\right)p\left\{X_r < \min\left(X_{\text{int\_PU}}, X_s\right)\right\}}{1-(1-P_{hI})P\left\{X_d < \min\left(X_{\text{int\_PU}}, X_{sr}\right)\right\}} \tag{37}$$

(a) For the case when X_s and X_d have a general pdf, in Appendix 3, it is shown that

$$P\{X_r < \min(X_{\text{int\_PU}}, X_s)\} = -\sum_{p\in\Omega_{X_r}} \mathbf{Res}_{s=p} \frac{\left[1-f^*_{X_s}\left(\lambda^{(P)}P_{\text{Int}}+s\right)\right]f^*_{X_r}(-s)}{\lambda^{(P)}P_{\text{Int}}+s} \tag{38}$$

and

$$P\{X_d < \min(X_{\text{int\_PU}}, X_{sr})\} = -\sum_{p\in\Omega X_d} \mathbf{Res}_{s=p} \frac{\left[1-f^*_{X_{sr}}\left(\lambda^{(P)}P_{\text{Int}}+s\right)\right]f^*_{X_d}(-s)}{\lambda^{(P)}P_{\text{Int}}+s} \tag{39}$$

Using (38) and (39) in (37), we have

$$\lambda_n = \frac{\lambda_n\left(1-P_b^{(s)}\right)\left(-\sum_{p\in\Omega_{X_r}} \mathbf{Res}_{s=p} \frac{\left[1-f^*_{X_s}\left(\lambda^{(P)}P_{\text{Int}}+s\right)\right]f^*_{X_r}(-s)}{\lambda^{(P)}P_{\text{Int}}+s}\right)}{1+(1-P_{hI})\sum_{p\in\Omega_{X_d}} \mathbf{Res}_{s=p} \frac{\left[1-f^*_{X_{sr}}\left(\lambda^{(P)}P_{\text{Int}}+s\right)\right]f^*_{X_d}(-s)}{\lambda^{(P)}P_{\text{Int}}+s}} \tag{40}$$

(b) For the particular case when X_s is exponentially distributed, in Appendix 3, it is shown that

$$P\{X_r < \min(X_{\text{int\_PU}}, X_s)\} = f^*_{X_r}\left(\mu+\lambda^{(P)}P_{\text{Int}}\right) \tag{41}$$

Using (41) in (37), we have

$$\lambda_h = \frac{\lambda n\left(1-P_b^{(s)}\right)f^*_{X_r}\left(\mu+\lambda^{(P)}P_{\text{Int}}\right)}{1+(1-P_{hI})\sum_{p\in\Omega_{X_d}} \mathbf{Res}_{s=p} \frac{\left[1-f^*_{X_{sr}}\left(\lambda^{(P)}P_{\text{Int}}+s\right)\right]f^*_{X_d}(-s)}{\lambda^{(P)}P_{\text{Int}}+s}} \tag{42}$$

For the sake of clarity and completeness, an alternative mathematical expression for calculation of the inter-cellular handoff arrival rate based on the cell departure rate is shown in Section 5, considering both UST and CDT exponentially distributed.

4.2 Forced call termination probability for secondary users

In this section, considering that UST is exponentially distributed and CDT is generally distributed, a closed analytical expression for the forced call termination probability in CRCNs is obtained. In mobile communication networks, forced call termination is due to two fundamental features: resource insufficiency and link unreliability [9]. Without loss of generality, in the following analysis, forced call termination probability due to link unreliability because of the propagation impairments is ignored. Instead, due to the nature of CRNs, a new type of forced call termination is introduced: forced termination due to intra-cellular handoff failure triggered by the arrival of a PU.

Note that $P_{\text{Int}} = P_0P_{hi}$ gives the interruption probability of a particular SU's call due to the arrival of a PU, where P_0 is the probability that the SU's call of interest occupies the claimed PU's resources and P_{hi} represents the probability of intra-cell handoff failure (due to either that an interrupted SU cannot find available resources to perform spectrum handoff or spectrum handoff is not employed). It is important to notice that when spectrum handoff is not considered $P_{hi} = 1$. In order to find the forced call termination probability for SUs, the main reasons for this are identified as follows: (a) when a SU attempts a handoff procedure as it leaves its current cell and there are no available resources in the target cell (which occurs with probability P_{ft}^H) and (b) when an interruption occurs due to an arrival of a PU that requires the resources used by the SU (which occurs with probability P_{ft}^{Int}) and no available channels there exist in the system. First, P_{ft}^H is studied in detail. A new call (handoff call) requires a handoff when its residual cell dwell (cell dwell) time in the current cell is smaller than both its unencumbered service (residual unencumbered service) time and the unencumbered interruption time. Let us consider that a particular handoff call fails with probability P_{hI}. As such, the forced call termination probability due to an inter-cellular handoff attempt failure is expressed as

$$\begin{aligned} P_{ft}^H = {} & P\left\{X_r < \min\left(X^{(0)}_{\text{int\_PU}}, X_s\right)\right\}P_{hI} \\ & + P\left\{X_r < \min\left(X^{(0)}_{\text{int\_PU}}, X_s\right), X_d^{(1)} \right. \\ & \left. < \min\left(X^{(1)}_{\text{int\_PU}}, X_s - X_r\right)\right\}(1-P_{hI})P_{hI} \\ & + P\left\{X_r < \min\left(X^{(0)}_{\text{int\_PU}}, X_s\right), X_d^{(1)} \right. \\ & \left. < \min\left(X^{(1)}_{\text{int\_PU}}, X_s - X_r\right), X_d^{(2)} < \min \right. \\ & \left. \times\left(X^{(2)}_{\text{int\_PU}}, X_s - X_r - X_d^{(1)}\right)\right\}(1-P_{hI})^2P_{hI} + \ldots \end{aligned} \tag{43}$$

Since here X_s is assumed to be exponentially distributed, using the memory-less property and considering that random variables $X_d^{(i)}\left\{X^{(j)}_{\text{int\_PU}}\right\}$ (for i = 1, 2,...) {for j = 0, 1, ...} are *i.i.d.*, we have

$$P_{ft}^H = P\{X_r < \min(X_{\text{int\_PU}}, X_s)\} P_{hI}\frac{1}{1-P\{X_d < \min(X_{\text{int\_PU}}, X_s)\}(1-P_{hI})} \tag{44}$$

In Appendix 3, it is shown that

$$P\{X_r < \min(X_{\text{int\_PU}}, X_s)\} = f^*_{X_r}\left(\mu + \lambda^{(P)} P_{\text{Int}}\right) \tag{45}$$

and

$$P\{X_d < \min(X_{\text{int\_PU}}, X_s)\} = f^*_{X_d}\left(\mu + \lambda^{(P)} P_{\text{Int}}\right) \tag{46}$$

Using (45) and (46) in (44), we have

$$P_{ft}^{H} = \frac{P_{hI} f^*_{X_r}\left(\mu + \lambda^{(P)} P_{\text{Int}}\right)}{1-(1-P_{hI}) f^*_{X_d}\left(\mu + \lambda^{(P)} P_{\text{Int}}\right)} \tag{47}$$

Now, P_{ft}^{Int} is studied in detail. A new call (handoff call) is terminated due to a PU arrival when the unencumbered interruption time of such user is smaller than both its residual cell dwell (cell dwell) time in the current cell and to the residual service time. Hence, it can be expressed as

$$\begin{aligned} P_{ft}^{\text{Int}} &= P\left\{X^{(0)}_{\text{int\_PU}} < \min\ (X_r,\ X_s)\right\} \\ &\quad + P\{X_r < \min\left(X^{(0)}_{\text{int\_PU}}, X_s\right), X^{(1)}_{\text{int\_PU}} \\ &\quad < \min\ \left(X^{(1)}_{d}, X_s - X_r\right)\}(1-P_{hI}) \\ &\quad + P\{X_r < \min\ \left(X^{(0)}_{\text{int\_PU}},\ X_s\right),\ X^{(1)}_{d} \\ &\quad < \min\ \left(X^{(1)}_{\text{int\_PU}},\ X_s - X_r\right),\ X^{(2)}_{\text{int\_PU}} \\ &\quad < \min\ \left(X^{(2)}_{d},\ X_s - X_r - X^{(1)}_{d}\right)\}(1-P_{hI})^2 + \ldots \end{aligned} \tag{48}$$

When X_s is assumed to be exponentially distributed, using the memory-less property and considering that the variables $X_d^{(i)}\left\{X^{(j)}_{\text{int\_PU}}\right\}$ (for i = 1, 2, ...) {for j = 0, 1, ...} are *i.i.d.*, we have

$$\begin{aligned} P_{ft}^{\text{Int}} &= P\{X_{\text{int\_PU}} < \min(X_r, X_s)\} \\ &\quad + \frac{(1-P_{hI}) P\{X_r < \min(X_{\text{int\_PU}}, X_s)\} P\{X_{\text{int\_PU}} < \min(X_d, X_s)\}}{1-(1-P_{hI}) P\{X_d < \min(X_{\text{int\_PU}}, X_s)\}} \end{aligned} \tag{49}$$

In Appendix 3, it is shown that

$$P\{X_{\text{int\_PU}} < \min(X_r,\ X_s)\} = \frac{\lambda^{(P)} P_{\text{Int}}\left[1 - f^*_{X_r}\left(\mu + \lambda^{(P)} P_{\text{Int}}\right)\right]}{\mu + \lambda^{(P)} P_{\text{Int}}} \tag{50}$$

$$P\{X_r < \min(X_{\text{int\_PU}}, X_s)\} = f^*_{X_r}\left(\mu + \lambda^{(P)} P_{\text{Int}}\right) \tag{51}$$

$$P\{X_{\text{int\_PU}} < \min\ (X_d,\ X_s)\} = \frac{\lambda^{(P)} P_{\text{Int}}\left[1 - f^*_{X_d}\left(\mu + \lambda^{(P)} P_{\text{Int}}\right)\right]}{\mu + \lambda^{(P)} P_{\text{Int}}} \tag{52}$$

and

$$P\{X_d < \min(X_{\text{int\_PU}}, X_s)\} = f^*_{X_d}\left(\mu + \lambda^{(P)} P_{\text{Int}}\right) \tag{53}$$

Using (50)–(53) in (49) and simplifying, we have

$$\begin{aligned} P_{ft}^{\text{Int}} &= \frac{\lambda^{(P)} P_{\text{Int}}\left(1 - f^*_{X,}\left(\mu + \lambda^{(P)} P_{\text{Int}}\right)\right)}{1-(1-P_{hI}) f^*_{X_d}\left(\mu + \lambda^{(P)} P_{\text{Int}}\right)} \\ &\quad + \frac{(1-P_{hI}) f^*_{X,}\left(\mu + \lambda^{(P)} P_{\text{Int}}\right) \lambda^{(P)} P_{\text{Int}}\left[1 - f^*_{X_d}\left(\mu + \lambda^{(P)} P_{\text{Int}}\right)\right]}{\left(\mu + \lambda^{(P)} P_{\text{Int}}\right)\left[1-(1-P_{hI}) f^*_{X_d}\left(\mu + \lambda^{(P)} P_{\text{Int}}\right)\right]} \end{aligned} \tag{54}$$

Using the fact that $f^*_{X_r}\left(\mu + \lambda^{(P)} P_{\text{Int}}\right) = \eta\left[1 - f^*_{X_d}\left(\mu + \lambda^{(P)} P_{\text{Int}}\right)\right] / \left(\mu + \lambda^{(P)} P_{\text{Int}}\right)$, (54) can be rewritten as

$$\begin{aligned} P_{ft}^{\text{Int}} = \lambda^{(P)} P_{\text{Int}} \Bigg(& \frac{\left(\lambda^{(P)} P_{\text{Int}} + \mu - \eta P_{hI}\right)}{\left(\mu + \lambda^{(P)} P_{\text{Int}}\right)^2 \left[1-(1-P_{hI}) f^*_{X_d}\left(\mu + \lambda^{(P)} P_{\text{Int}}\right)\right]} \\ & - \frac{\left[\left(\lambda^{(P)} P_{\text{Int}} + \mu\right)(1-P_{hI}) - \eta P_{hI}\right] f^*_{X_d}\left(\mu + \lambda^{(P)} P_{\text{Int}}\right)}{\left(\mu + \lambda^{(P)} P_{\text{Int}}\right)^2 \left[1-(1-P_{hI}) f^*_{X_d}\left(\mu + \lambda^{(P)} P_{\text{Int}}\right)\right]} \Bigg) \end{aligned} \tag{55}$$

Thus, the global forced call termination probability is given by

$$\begin{aligned} P_{ft} &= \frac{P_{hI} f^*_{X_r}\left(\mu + \lambda^{(P)} P_{\text{Int}}\right)}{1-(1-P_{hI}) f^*_{X_d}\left(\mu + \lambda^{(P)} P_{\text{Int}}\right)} \\ &\quad + \frac{\lambda^{(P)} P_{\text{Int}}\left[1 - f^*_{X_r}\left(\mu + \lambda^{(P)} P_{\text{Int}}\right)\right]}{\mu + \lambda^{(P)} P_{\text{Int}}} \\ &\quad + \frac{(1-P_{hI}) f^*_{X_r}\left(\mu + \lambda^{(P)} P_{\text{Int}}\right) \lambda^{(P)} P_{\text{Int}}\left[1 - f^*_{X_d}\left(\mu + \lambda^{(P)} P_{\text{Int}}\right)\right]}{\left(\mu + \lambda^{(P)} P_{\text{Int}}\right)\left[1-(1-P_{hI}) f^*_{X_d}\left(\mu + \lambda^{(P)} P_{\text{Int}}\right)\right]} \end{aligned} \tag{56}$$

Finally, it is important to mention that the methodology proposed in this section to derive the forced call termination probability turns mathematically intractable when non-exponential distributions for the UST are considered. Nonetheless, when phase-type probability distributions are considered to model the UST, the call forced termination probability can be calculated as the ratio of the rate of forced termination calls

and the rate of accepted calls as it is done in [9]. However, in this case, it is necessary to calculate a quantity which is closely related to the steady-state probabilities (as in [9, 11]) and no closed analytical expressions can be obtained. For the sake of clarity and completeness, an alternative mathematical expression for the forced call termination probability (computed as the ratio of the rate of forced termination calls and the rate of accepted calls) is presented in the next section, considering both UST and CDT exponentially distributed.

5 Teletraffic analysis

In this section, the queuing analysis for the performance evaluation of mobile CRCNs with FR-HDC traffic is developed. For the sake of simplicity, it is considered that both UST and CDT of SUs are exponentially distributed.[7] Also, it is assumed that the primary channel holding time is exponentially distributed with mean $1/\mu^{(P)}$. To maximize system Erlang capacity and for the adequate and fair performance comparison of the different considered scenarios, fractional channel reservation [1, 38, 39] to prioritize both intra (due to spectrum handoff)- and inter (due to users' mobility)-cell handoff call attempts over new call requests is considered in the call admission control strategy. To this end, a number of $\lfloor r \rfloor + 1$ sub-bands is reserved with probability $p = r - \lfloor r \rfloor$ and a number of $\lfloor r \rfloor$ sub-bands is reserved with probability $(1 - p)$. Thus, a bi-dimensional birth and death process is required for modeling this system. Each state variable is denoted by x_i (for $i = 0, 1$). x_0 represents the number of primary users, and x_1 represents the number of SUs. To simplify mathematical notation, the following vector of state variables is defined $\mathbf{x} = (x_0, x_1)$. k represents the number of active cognitive users that have to relinquish their respective sub-channel due to the arrival of a PU service request. As explained in [36], when no spectrum handoff is used, k is a random variable ($\mathbf{k}$), and on the other hand, when spectrum handoff is used, k is a deterministic value. Thus, the probability mass function (pmf) of the random variable $\mathbf{k}$, when spectrum handoff is not used, is given by [36]

$$p_{\mathrm{NSH}}(\mathbf{x}, \mathbf{k} = k) = \frac{\binom{N}{k}\binom{N(M-(x_0+1))}{x_1-k}}{\binom{N(M-x_0)}{x_1}} \tag{57}$$

for $k = 0, 1, \ldots, \min(x_1, N)$ and, when spectrum handoff is used, it is given by

$$p_{\mathrm{SH}}(\mathbf{x}, \mathbf{k} = k) = \begin{cases} 1 \ ; (M-1)N < x_1 + Nx_0 \leq MN \\ 0; \text{otherwise} \end{cases} \tag{58}$$

for $k = x_1 + N(x_0 + 1) - MN$. The valid state space Ω is

$$\Omega = \{\mathbf{x} | 0 \leq x_0 \leq M, 0 \leq x_1 \leq MN - Nx_0\}$$

5.1 System without spectrum handoff

When no spectrum handoff is allowed, if a PU decides to access a primary channel, all SUs using that channel must relinquish their transmission immediately. Let us represent by $r_{\mathbf{xy}}$ and $\mathbf{e}_i$ the transition rate from state $\mathbf{x}$ to state $\mathbf{y}$ ($\mathbf{x} \in \Omega$) and a two-dimensional vector with position i set to 1 and the other position set to 0, respectively. Then, the steady-state probabilities balance equation can be written as

$$P(\mathbf{x}) \sum_{\forall \mathbf{y} \in \Omega} r_{\mathbf{xy}} = \sum_{\forall \mathbf{y} \in \Omega} P(\mathbf{y}) r_{\mathbf{xy}} \ \ \forall \mathbf{x} \in \Omega \tag{59}$$

where $P(\mathbf{x})$ is the state $\mathbf{x}$ stationary probability and the transition rate $r_{\mathbf{xy}}$ from states $\mathbf{x}$ to $\mathbf{y}$ is given by

$$r_{\mathbf{xy}} = \begin{cases} a_0(\mathbf{x})\lambda^{(P)} & ; \mathbf{y} = \mathbf{x} + \mathbf{e}_0 - k\mathbf{e}_1; \quad \mathbf{y} \in \Omega \\ \lambda_n + \lambda_h & ; \mathbf{y} = \mathbf{x} + \mathbf{e}_1; \ x_1 \geq 0; \ Nx_0 + x_1 < MN - \lfloor r \rfloor - 1 \\ (1-p)\lambda_n + \lambda_h & ; \mathbf{y} = \mathbf{x} + \mathbf{e}_1; \ x_1 \geq 0; \ Nx_0 + x_1 = MN - \lfloor r \rfloor - 1 \\ \lambda_h & ; \mathbf{y} = \mathbf{x} + \mathbf{e}_1; x_1 \geq 0; \ MN > Nx_0 + x_1 > MN - \lfloor r \rfloor - 1 \\ x_0\mu^{(P)} & ; \mathbf{y} = \mathbf{x} - \mathbf{e}_0; \quad \mathbf{y} \in \Omega \\ x_1(\mu + \eta) & ; \mathbf{y} = \mathbf{x} - \mathbf{e}_1; \quad \mathbf{y} \in \Omega \\ 0 & \text{otherwise} \end{cases} \tag{60}$$

where $a_0(\mathbf{x}) = p_{\mathrm{NSH}}(\mathbf{x},\mathbf{k})$. The state transition diagram of this system is shown in Fig. 4. The values of $P(\mathbf{x})$ are obtained from (59) and the normalization equation.

It is important to note that the previous teletraffic analysis represents an approximation approach for the performance evaluation of the considered system. Specifically, the steady-state probabilities are obtained considering that the interruption time of SUs' calls due to the arrival of PUs follows a Poisson process. As

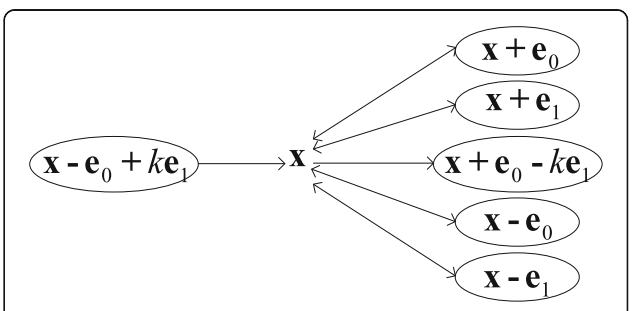

Fig. 4 State transition diagram

proven in Appendix 1, this is not true. However, this approximation renders accurate numerical results for most of the scenarios and performance metrics of interest, as shown in Section 6.

Then, the inter-cellular handoff failure probability P_{hI} and new call blocking probability $P_b^{(S)}$ can be computed as follows

$$P_{hI} = P_b^{(S)} = \sum_{x_0=0}^{M} P(x_0, MN - Nx_0) \tag{61}$$

When no spectrum handoff is considered, a random number of **k** cognitive users will be forced to terminate their service due to the arrival of a PU in a specific primary channel which is occupied by **k** SUs. The interruption probability due to the arrival of PU, P_{Int}, is given by

$$P_{\text{Int}} = \frac{\sum_{x_0=0}^{M}\sum_{x_1=1}^{MN-Nx_0} \Gamma(\mathbf{x})P(\mathbf{x})}{\sum_{x_0=0}^{M}\sum_{x_1=1}^{MN-Nx_0} P(\mathbf{x})} \tag{62}$$

where

$$\Gamma(\mathbf{x}) = \sum_{\substack{k=0 \\ x_1 + Nx_0 \le N(M-1)}}^{min(x_1,N)} kp_{\text{NSH}}(\mathbf{x},\mathbf{k}) + \sum_{\substack{k = x_1 + N(x_0+1) - MN \\ N(M-1) < x_1 + Nx_0 \le MN}}^{\min(x_1,N)} kp_{\text{NSH}}(\mathbf{x},\mathbf{k}) \tag{63}$$

Considering (42) and the fact that CDT is considered exponentially distributed in this section, the inter-cellular handoff rate λ_h can be calculated as

$$\lambda_h = \frac{\eta\lambda_n\left(1 - P_b^{(s)}\right)}{\eta P_{hI} + \mu + \lambda^{(P)} P_{\text{Int}}} \tag{64}$$

Alternatively, inter-cellular handoff rate λ_h can be calculated using the cell departure rate as follows

$$\lambda_h = \sum_{x_0=0}^{M} \sum_{x_1=0}^{MN-Nx_0} x_1 \eta P(\mathbf{x})$$

The fixed point iteration method is employed to iteratively calculate the inter-cellular handoff rate as explained in [40].

Considering exponentially distributed cell dwell time, the forced call termination probability given by (56) can be written as

$$P_{ft} = \frac{\eta P_{hI} + \lambda^{(P)} P_{\text{Int}}}{\eta P_{hI} + \mu + \lambda^{(P)} P_{\text{Int}}} \tag{65}$$

Notice that (65) is a closed-form approximated expression to compute forced call termination probability. Equation (65) is an approximated expression in the sense that it was derived in Section 4 considering that call interruption times follow a Poisson process. Moreover, expression (65) depends on P_{hI} and P_{Int}, which are derived in this section considering, also, that call interruption process is a Poisson one. Thus, we can say that (65) is based on a "double approximation." Nonetheless, the importance of (65) lies on the fact that it depends on parameters that can be easily obtained from statistics that can be collected in real networks.

An alternative expression for calculating forced call termination probability can be obtained as the ratio of the rate of forced terminated calls and the rate of accepted calls. Mathematically,

$$P_{ft} = \frac{\lambda^{(P)} \sum_{x_0=0}^{M-1} \sum_{x_1=N(M-1)-Nx_0}^{MN} [N(x_0+1) + x_1 - MN] P(\mathbf{x})}{\lambda_n\left(1 - P_b^{(S)}\right)} + \frac{\lambda_h P_{hI}}{\lambda_n\left(1 - P_b^{(S)}\right)} \tag{66}$$

Notice that for the computation of (66), it is needed to know the steady-state probabilities. However, compared to (65), the unique source of imprecision of (66) is the fact that steady-state probabilities are derived considering that call interruption process is a Poisson one.

5.2 System with spectrum handoff

When spectrum handoff is considered, interrupted SUs are allowed to move to other vacant channels (if available). It is not difficult to observe that when spectrum handoff is used, $a_0(\mathbf{x}) = p_{\text{SH}}(\mathbf{x},\mathbf{k})$ in Eq. (58).

In this case (i.e., for cognitive radio networks with spectrum handoff), the mathematical expressions for the new call blocking and forced call termination probabilities and the inter-cellular handoff rate remain unchanged relative to the case when no spectrum handoff is considered; they are given by (61), (65), and (64), respectively. However, in this case, the interruption probability due to the arrival of PU, P_{Int}, is given by

$$P_{\text{Int}} = \frac{\sum_{x_0=0}^{M} \sum_{x_1=1}^{MN-Nx_0} \frac{(x_1+N(x_1+1)-MN)}{x_1} P(\mathbf{x})}{\sum_{x_0=0}^{M} \sum_{x_1=1}^{MN-Nx_0} P(\mathbf{x})} \quad (67)$$

5.3 Erlang capacity maximization

The maximum Erlang capacity is computed as the maximum value of the offered traffic for which all the QoS requirements are still met. Maximum Erlang capacity is obtained by optimizing the number of reserved channels to prioritize intra- and inter-cell handoff call attempts over new call requests. The optimal value of the number of reserved channels is systematically searched by using the fact that new call blocking (handoff failure) probability is a monotonically increasing (decreasing) function of the number of reserved channels. Once a value of the number of reserved channels for which the new call blocking probability and/or handoff failure probability achieves its maximum acceptable value is found, another offered traffic load is tested. The capacity maximization procedure ends when both the new call blocking probability and forced call termination probability achieve their maximum acceptable values.

6 Performance evaluation

The goal of the numerical evaluations presented in this section is to verify the applicability as well as the accuracy and robustness of our developed mathematical models. In particular, in this section, numerical results for performance evaluation of mobile CRCN in the presence of both intra-cellular e inter-cellular handoff mechanisms are shown. The analytical numerical results presented in this section were verified by a wide set of discrete-event computer simulation results for a variety of evaluation scenarios. Part of this numerical validation is shown in our previous work [23], as commented in Section 6.2. In Section 6.1, channel holding time statistics are analyzed, while in Section 6.2, the effect of secondary session interruption due to the arrival of PUs on the performance of CRCN is investigated. In this section, we define the mobility parameter as the ratio between the mean value of the UST and the mean value of the CDT, that is, the mobility parameter is given by η/μ.

6.1 Influence of the interruption probability and the probability distributions used to model the cell dwell and unencumbered service times on the channel holding time statistics

In this section, numerical results are presented to investigate the extent by which the probability distributions of both CDT and UST as well as the interruption probability (P_{Int}) affect the statistics of both new call channel holding time (CHTn) and handoff call channel holding time (CHTh). Different phase-type distributions to model CDT and UST are used. Remember that the random variable used to model the elapsed time between call interruptions is approximated by an exponential distribution with parameter $P_{\text{Int}}\lambda^{(P)}$. As it is explained in the last paragraph of Section 3, the statistics of the CHTn and CHTh are obtained using (12) and (35), respectively.

Figures 5, 6, and 7 present the mean, coefficient of variation (CoV), and skewness (Sk) of the CHTn (represented by solid lines) and CHTh (represented by dashed lines)

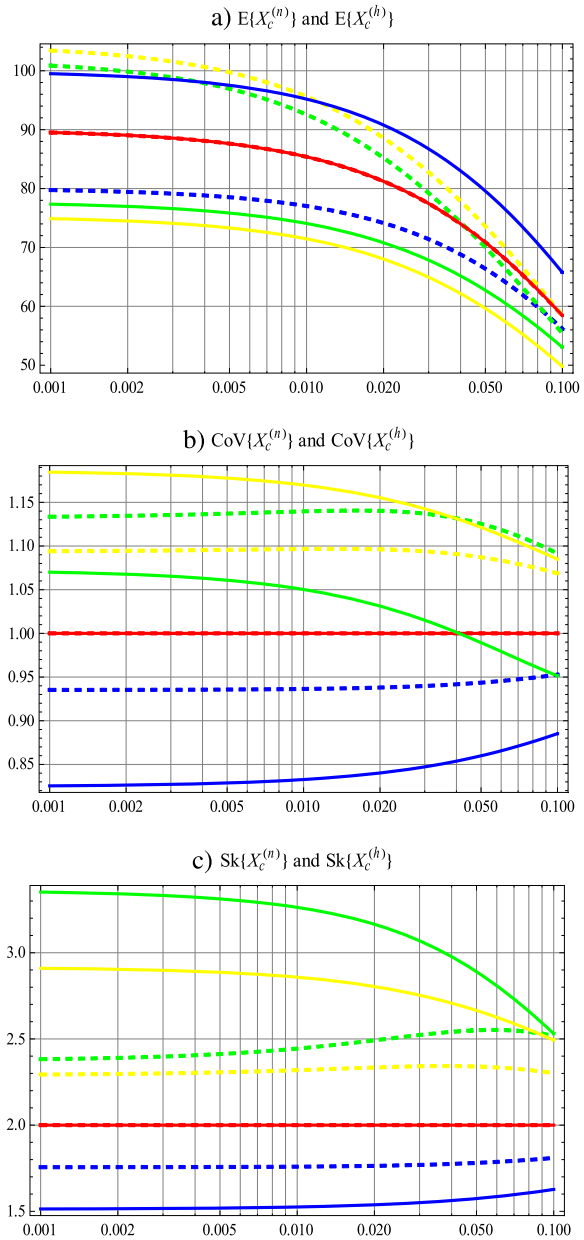

Fig. 5 a–c CHT statistics as a function of the interruption probability for different distributions of the UST when CDT is exponentially distributed. In this figure, *red*, *blue*, *yellow*, and *green lines* represent the scenarios where the UST is exponentially, Erlang, hyper-exponentially of order 2, and hyper-Erlang of order (2, 2) distributed, respectively. *Solid-lines* (*dashed-lines*) corresponds to CHTn (CHTh) statistics

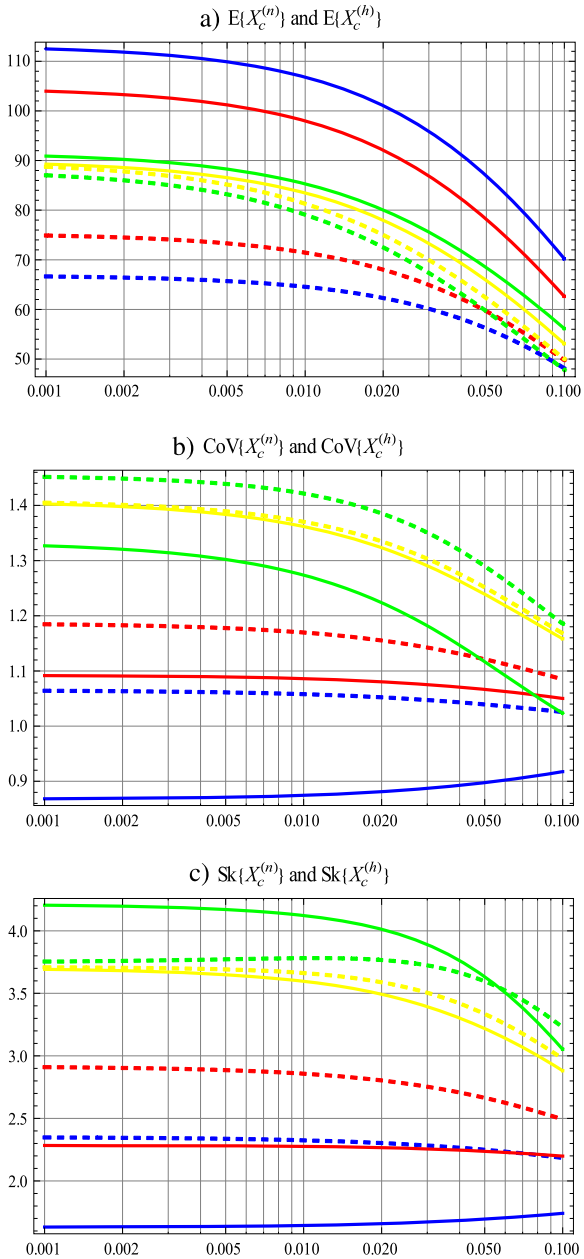

Fig. 6 a–c CHT statistics as a function of the interruption probability for different distributions of the UST when CDT is hyper-exponentially distributed. In this figure, *red*, *blue*, *yellow*, and *green lines* represent the scenarios where the UST is exponentially, Erlang, hyper-exponentially of order 2, and hyper-Erlang of order (2, 2) distributed, respectively. *Solid-lines* (*dashed-lines*) corresponds to CHTn (CHTh) statistics

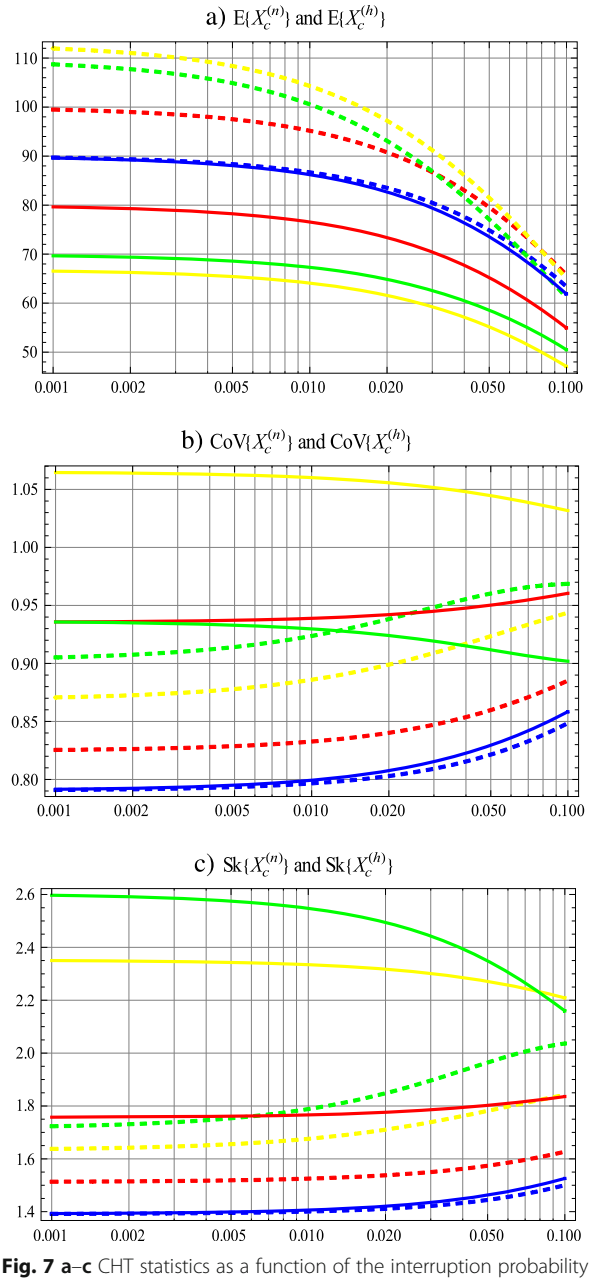

Fig. 7 a–c CHT statistics as a function of the interruption probability for different distributions of the UST when CDT is Erlang distributed. In this figure, *red*, *blue*, *yellow*, and *green lines* represent the scenarios where the UST is exponentially, Erlang, hyper-exponentially of order 2, and hyper-Erlang of order (2, 2) distributed, respectively. *Solid-lines* (*dashed-lines*) corresponds to CHTn (CHTh) statistics

versus the interruption probability P_{Int} for different distributions of the UST; specifically, in Figs. 5, 6, and 7, red, blue, yellow, and green lines represent, respectively, the scenarios where the UST is exponentially, Erlang, hyper-exponentially of order 2, and hyper-Erlang of order (2, 2) distributed. Referring to the CDT, Figs. 5, 6, and 7 assume that the CDT is exponentially, hyper-exponentially of order 2, and Erlang distributed, respectively. Referring to the different probability distributions considered in this section, it is important to point out that the exponential distribution is completely characterized by its mean value, the Erlang distribution is completely characterized by its first two moments (i.e., mean value and coefficient of variation), and the hyper-exponential and hyper-Erlang distributions are both completely characterized by their first

Table 3 Mean of the CHTn for different distributions of the UST when CDT is exponentially distributed

P_{Int}	UST distribution							
	Exp-Neg		Erlang		Hyper-exponential order 2		Hyper-Erlang (2,2)	
	Simulation	Analytical	Simulation	Analytical	Simulation	Analytical	Simulation	Analytical
0.001	89.17	89.52	99.15	99.5	75.55	74.89	77.22	77.35
0.02	81.04	81.23	90.81	90.78	68.36	68.02	70.91	70.79
0.05	70.68	70.87	79.42	79.57	59.34	59.65	62.84	62.73
0.1	58.21	58.44	65.67	65.74	49.98	49.79	53.25	53.06

three moments (i.e., mean value, coefficient of variation, and skewness). As long as possible, the same values of the first three moments of the different probability distributions are considered. In all the plots of this section, it is considered that $P_{hI} = 0.01$ and the following representative values are considered: $E\{X_s\} = 1/\mu = 180$ s, $\text{CoV}\{X_s\} = 1.58$, $\text{Sk}\{X_s\} = 3.54$, $E\{X_d\} = 1/\eta = 180$ s, $\text{CoV}\{X_d\} = 1.58$, $\text{Sk}\{X_d\} = 3.54$, and $\lambda^{(P)} = 0.06$ arrivals per second. Notice that, in this scenario, the mobility parameter (i.e., η/μ) equals 1.0, which corresponds to a relatively high users' mobility scenario. It is important to note that the analytical results have been compared to Monte Carlo simulation results in order to validate our numerical results. In Tables 3, 4, and 5, we can see a perfect match between these two models (analytical and simulation) for each scenario considered in this work.

Several interesting observations can be extracted from Figs. 5, 6, and 7. For instance, from Fig. 5, it is observed that, when CDT and UST are modeled by the (unrealistic) exponential distribution and for any value of the interruption probability, the corresponding mean, CoV, and Sk of both CHTn and CHTh have the same value (this scenario is represented by the solid-red and dashed-red lines in Fig. 5). This is an expected behavior that validates our mathematical formulation and can be explained as follows. Due to the memory-less property of the exponential distribution, when CDT (UST) is exponentially distributed, the residual CDT (residual UST) is also exponentially distributed with the same parameter [12]. Thus, the random variables that represent CHTn and CHTh (whose probability distributions are given by Eqs. (12) and (35), respectively) are also exponentially distributed with the same expected value, and therefore, the CoV and Sk are, respectively, 1 and 2 for both CHTn and CHTh. Also, from Figs. 5a, 6a, and 7a, it is observed that the mean value of both CHTn and CHTh is a monotonically decreasing function of the interruption probability. It is an intuitively understandable behavior due to the fact that as the probability of interruption increases, more ongoing secondary calls are prematurely terminated in detrimental of the mean value of both CHTn and CHTh.

However, the most relevant result that can be extracted from the plots presented in Figs. 5, 6, and 7 is the fact that the CHT statistics are highly sensitive to the distribution type of both CDT and UST. To exemplify this, let us quantify the impact of the distribution type used to model the UST on the statistics of the CHTn (the behavior of the CHTn is represented by the solid lines in Figs. 5, 6, and 7). To this end, let us consider the case when both the UST and CDT are exponentially distributed as the reference case (this scenario is represented by the red solid-line in Fig. 5). Thus, considering the scenario where $P_{\text{Int}} = 0.01$, Fig. 5a shows that (with respect to the reference case) the mean value of the CHTn increases 11.5% when the UST is Erlang distributed and decreases 16.3 and 13.3% when the UST is hyper-exponentially and hyper-Erlang distributed, respectively. Under the same scenario, Fig. 5b shows that (with respect to the reference case) the CoV of CHTn decreases 16.7% when the UST is Erlang distributed and increases 17 and 5% when the UST is hyper-exponentially and hyper-Erlang distributed, respectively. Similarly, Fig. 5c shows that (with respect to the reference case) the skewness of the CHTn decreases 23.7% when the UST is Erlang distributed and increases 42.9 and 63% when the UST is hyper-exponentially and hyper-Erlang distributed, respectively. Similar results are obtained when the CHTh is considered.

Table 4 Coefficient of variation of the CHTn for different distributions of the UST when CDT is exponentially distributed

P_{Int}	UST distribution							
	Exp-Neg		Erlang		Hyper-exponential order 2		Hyper-Erlang (2,2)	
	Simulation	Analytical	Simulation	Analytical	Simulation	Analytical	Simulation	Analytical
0.001	1	1	0.826	0.825	1.18	1.18	1.07	1.07
0.02	1	1	0.84	0.84	1.16	1.155	1.04	1.03
0.05	1	1	0.86	0.86	1.12	1.12	0.99	0.99
0.1	1	1	0.88	0.885	1.09	1.09	0.95	0.95

Table 5 Skewness of the CHTn for different distributions of the UST when CDT is exponentially distributed

P_{Int}	UST distribution							
	Exp-Neg		Erlang		Hyper-exponential order 2		Hyper-Erlang (2,2)	
	Simulation	Analytical	Simulation	Analytical	Simulation	Analytical	Simulation	Analytical
0.001	1.99	2	1.49	1.51	2.98	2.90	3.22	3.35
0.02	2.02	2	1.52	1.53	2.91	2.80	3.25	3.16
0.05	1.99	2	1.56	1.57	2.71	2.66	2.74	2.89
0.1	2.00	2	1.63	1.62	2.47	2.49	2.55	2.53

On the other hand, Figs. 5a, 6a, and 7a show that, for a given CDT probability distribution and for a given value of the interruption probability, the quantitative difference between the mean value of the CHTn when the UST is hyper-exponentially distributed and the mean value of the CHTn when the UST is hyper-Erlang distributed is small but not negligible (differences not greater than 6.6% are found). Referring to the CoV {skewness} of the CHTn, Figs. 5b, c, 6b, c, and 7b, c show important differences between the case when the UST is hyper-exponential and the case when the UST is hyper-Erlang distributed (differences up to 12.75 and 15.20% are observed for the CoV and Sk, respectively). Similar results are obtained when the CHTh is considered. Due to the fact that both distributions (i.e., hyper-exponential and hyper-Erlang) for modeling the UST have the same first three standardized moments, we conclude that the (not negligible) quantitative difference among the mean value, CoV, and Sk of both CHTn and CHTh when the UST is hyper-exponentially distributed compared to the case when the UST is hyper-Erlang distributed is due to moments higher than the third one. Analyzing the impact of moments of UST (and CDT) higher than the third one on channel holding time statistics represents a topic of our current research.

Now let us study the impact of the variability of both UST and CDT on CHT statistics. To this end, it is important to notice that the CoV of the Erlang, exponential, and hyper-exponential/hyper-Erlang distributions are, respectively, smaller than 1, equal to 1, and larger than 1. Thus, the variability of UST increases as its probability distribution moves from the Erlang to the exponential and from the exponential to the hyper-exponential/hyper-Erlang. The same observation applies for the CDT. Considering this fact, the following observation can be extracted from Figs. 5, 6, and 7. Figures 5, 6, and 7 show that, in general terms, as the variability of the UST (CDT) increases (decreases), the mean value of the CHTn decreases and at the same time the mean value of the CHTh increases. This behavior can be explained as follows. First, note that as the CoV of UST (CDT) increases, the variability of UST (CDT) increases; that is, the values of UST (CDT) spread out over a larger range with respect to its mean value. Consequently, the service time (cell residence time) of calls that end their service in the cell where they were originated is, in general, considerable smaller (greater) than the mean UST (CDT), resulting in a diminution (increase) on the mean value of the CHTn. On the other hand, the service time (cell residence time) of calls that are handed off to another cell is, in general, considerably greater (lower) than the mean UST (CDT), resulting in an augment (diminution) on the mean value of the CHTh. The combined effects of these facts lead us to the behavior explained above and observed in Figs. 5, 6, and 7. Many others interesting observations can be extracted from Figs. 5, 6, and 7; however, the most important ones are summarized as follows. The mean values of both CHTn and CHTh are strongly sensitive to the interruption probability. For instance, when the UST is hyper-Erlang distributed and the CDT is exponential distributed (notice that this scenario corresponds to the green lines of Fig. 5a), the mean value of CHTn (CHTh) decreases from 77.35 to 53.057 s (101 to 55.4 s) as the interruption probability goes from 0.001 to 0.1. Similar behaviors are observed when the CDT is modeled by either an Erlang or a hyper-exponential distribution. Also, from Figs. 5, 6, and 7, it is evident that the first three moments of both CHTn and CHTh are highly sensitive to the probability distribution of both CDT and UST. Thus, selecting a suitable model that effectively captures the realistic statistics of both CDT and UST is of paramount importance when analyzing the performance of mobile cognitive radio cellular networks.

6.2 Effects of the secondary service time, users' mobility, and the primary channel utilization factor on system performance

In this section, the effects of the value of the mean secondary service time relative to the mean primary service time (hereafter called *relative service time*), mobility parameter (defined as the ratio between the mean service time and the mean cell residence time), the use or not of spectrum handoff (SH), and the primary channel utilization factor on the system Erlang capacity are evaluated. Additionally, the accuracy of the proposed approximate teletraffic model is evaluated for different evaluation scenarios. Specifically, four different scenarios

are considered: (S1) low mobility with small relative service time, (S2) low mobility with large relative service time, (S3) high mobility with small relative service time, and (S4) high mobility with large relative service time. Table 4 summarizes the values of the parameters used in these scenarios. Unless otherwise specified, the following values of system parameters were used for the numerical evaluations shown in this section: mean service time is $1/\mu^{(S)}$ = 1/0.82 s; as indicated in Table 6, two different values have been used for both the relative service time and mobility parameter, say, $\mu^{(P)}/\mu^{(S)}$ = {0.1, 1} and $\eta/\mu^{(S)}$ = {0.2, 1}, respectively; total number of identical primary channels per cell M = 3; the number of identical sub-channels per primary channel N = 6 (that is, non-homogeneous bandwidth of PU and SU channels are considered), including the possibility of interruption of multiple SUs.

The analytical numerical results presented in this subsection were verified by a wide set of discrete-event computer simulation results for a variety of evaluation scenarios. Part of this numerical validation is shown in our previous work [23]. Nevertheless, for clarity proposes and easy visualization and comparison of the different scenarios, simulation results for the metrics presented in Figs. 8 and 9 are omitted. Please note that the teletraffic analysis (and the correspondent considered system model) of Section 5.2 is identical to that developed in [23]. In this paper, new call blocking and forced call termination probabilities of secondary users are employed to obtain both the maximum Erlang capacity and the optimum number of reserved channels shown in Figs. 8 and 9, respectively. Figures 2 and 3 of [23] show simulation and analytical numerical results of new call blocking and forced call termination probabilities of secondary users as function of the mobility factor of both primary and secondary users with the secondary traffic load as parameter. From the curves presented in Figures 2 and 3 of [23], it is observed perfect agreement between analytical and simulation results. As perfect agreement between analytical and simulation results is observed for these probabilities in [23], no additional validation is needed for the analytical results presented in Figs. 8 and 9 of this paper. On the other hand, note that perfect agreement is observed between analytical and simulation results for all the evaluation scenarios shown in Fig. 10.

Table 6 Parameters for the considered scenarios

Scenario	Description	Mobility parameter ($\eta/\mu^{(S)}$)	Relative service time ($\mu^{(P)}/\mu^{(S)}$)
S1	Low mobility, small relative service time	0.2	0.1
S2	Low mobility, large relative service time	0.2	1
S3	High mobility, small relative service time	1	0.1
S4	High mobility, large relative service time	1	1

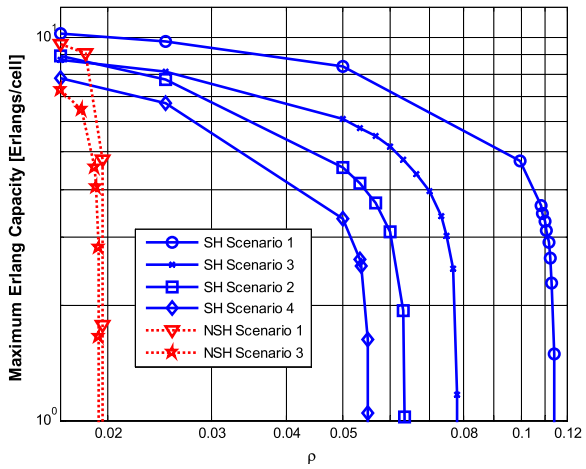

Fig. 8 Erlang capacity as a function of the utilization factor of the primary channels for the scenarios described in Table 6. Both spectrum handoff and non-spectrum handoff cases are considered for scenarios 1 and 3

Figure 8 depicts Erlang capacity as function of the primary channel utilization factor (defined as the ratio between the primary carried load and the total number of primary channels, i.e., $\rho = a_{c^{(P)}}/M$) for the different scenarios described in Table 6. Both spectrum handoff (SH) and non-spectrum handoff (NSH) cases are considered. Erlang capacity shown in Fig. 8 is obtained using the optimization procedure described in the last paragraph of Section 5.3. Specifically, the optimal number of reserved channels is computed in such a way that the system capacity is maximized, while the QoS requirements,

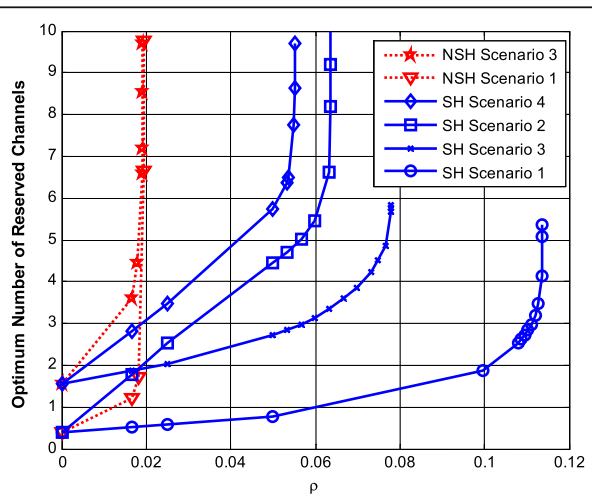

Fig. 9 Optimum number of reserved channels to achieve the Erlang capacity is shown in Fig. 8, as a function of the utilization factor of the primary channels for the scenarios described in Table 6. Both spectrum handoff and non-spectrum handoff are considered for scenarios 1 and 3

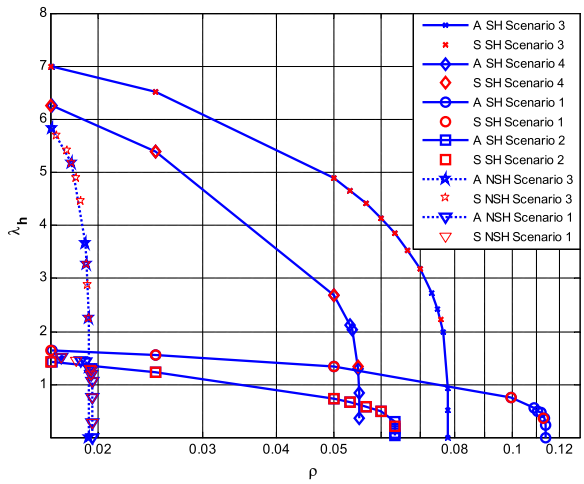

Fig. 10 Inter-cell handoff arrival rate for the Erlang capacity is shown in Fig. 8, as a function of the utilization factor of the primary channels for the scenarios described in Table 6. Both spectrum handoff and non-spectrum handoff are considered for scenarios 1 and 3

in terms of new call blocking and forced call termination probabilities, are achieved. New call blocking and forced call termination probabilities are evaluated using (61) and (66), respectively. Both of these probabilities are function of the interruption probability, which is evaluated using (62) and (67) for the NSH and SH cases, respectively. Maximum acceptable values of the new call blocking (P_{b_tr}) and forced call termination (P_{ft_tr}) probabilities are fixed to 2 and 0.2%, respectively.

From Fig. 8, it is observed that, for all the scenarios, as the utilization factor of primary channels (denoted by ρ) increases, system Erlang capacity decreases. This is an intuitively understandable result because as ρ increases, the average number of available channels for both new and (inter- and intra-) handed off secondary sessions decreases in detrimental of system capacity. Moreover, as ρ increases, more secondary calls are interrupted due to the arrival of primary sessions in detrimental of system performance. Let us consider, for example, the scenario S1 for the SH case. Figure 8 shows that as ρ moves from 0.0 (notice that this value of ρ corresponds to the conventional cellular system) to 0.1, Erlang capacity diminishes 52%.

Figure 8 also shows that there exists a critical value of the utilization factor of the primary channels (critical operational point) at which it is no longer possible to guarantee the QoS of the admitted secondary users (Erlang capacity abruptly decreases toward zero). This behavior is more evident for the NSH case. For instance, for the scenario S1, Fig. 8 indicates that this critical value is about 0.018 for the NSH case and it is about 0.106 for the SH case; that is, the critical operational point is increased about 488% by using spectrum handoff. From these results, we can see that the utilization factor of primary channels for which the Erlang capacity is zero when SH is enabled is $\rho = 0.106$ and when NSH is enabled is $\rho = 0.018$. As such, the utilization factor is increased as by $\Delta\rho = (0.106 - 0.018) = 0.088$. However, relative percentage difference to the case when NSH is being used is given by $\frac{100(0.106-0.018)}{0.018}\% = 488\%$. In other words, these results reveal that the use of spectrum handoff is essential for maximizing the arrival rate of PUs at which it is still possible to provide the QoS demanded by SUs. Similarly, Fig. 8 shows that the critical operational point decreases as either relative service time or mobility parameter increases. For instance, for the high mobility case (scenarios S3 and S4), the critical operational point decreases 30% as the relative service time moves from 0.1 (scenario S3) to 1.0 (scenario S4). On the other hand, for the large relative service time case (scenarios S2 and S4), the critical operational point decreases 13.12% as the mobility parameter goes from 0.2 (scenario S2) to 1.0 (scenario S4). This is because the utilization factor of primary channels for which the Erlang capacity is zero in scenarios S2 and S4 with SH is $\rho = 0.6346$ and $\rho = 0.5513$ for scenarios S2 and S4, respectively. Hence, there is an absolute decrease of $\Delta\rho = (0.6346 - 0.5513) = 0.0833$, but the relative percentage difference to the utilization factor of scenario S2 is $\frac{100(0.6346-0.5513)}{0.6346}\% = 13.12\%$. In general, Fig. 8 shows that Erlang capacity is more sensitive to the relative service time than to the mobility parameter. For instance, let us consider the scenario S1 for the SH case as the scenario of reference. Figure 8 shows that, for $\rho = 0.05$, Erlang capacity decreases 44% as the relative service time changes from 0.1 (scenario S1) to 1.0 (scenario S2), while Erlang capacity decreases 28% as the mobility parameter goes from 0.2 (scenario S1) to 1.0 (scenario S3). Figure 8 presents that for scenario S2, when the utilization factor of primary channels is $\rho = 0.05$, the Erlang capacity is 4.7 Erlangs. For scenario S1 for the same value of ρ, it has 8.4 Erlangs which corresponds to a reduction of $\frac{100(8.4-4.7)}{8.4}\% = 44.04\%$. In a similar way, for scenario S3, when $\rho = 0.05$, the Erlang capacity is 6.05 Erlangs. Hence, the Erlang capacity reduction relative to scenario S1 is $\frac{100(8.4-6.05)}{8.4}\% = 27.98\%$.

This behavior is due to the following two facts. First, the handoff arrival rate increases as the user mobility increases in detrimental of call forced termination probability. Thus, in order to achieve the required forced call termination probability (i.e., 0.2%), as the user mobility increases, more channels to prioritize intra- and inter-cell handoff call attempts over new call requests need to be reserved in detrimental of new call blocking

probability. Consequently, in order to achieve the required new call blocking probability (i.e., 2%), system Erlang capacity is sacrificed (mobility/capacity conversion [41]). Second, increasing the relative service time implies that the mean value of the secondary service time relative to the mean value of the primary service time increases. In this sense, as the relative service time increases (while the utilization factor of the primary channels remains unchanged), it is more likely that an ongoing secondary call is interrupted due to the arrival of primary sessions in detrimental of forced call termination probability. Because of its larger duration, each secondary call is exposed to a larger number of interruptions. Thus, as explained above, in order to guarantee the required QoS, in terms of the forced call termination, more channels need to be reserved in detrimental of the maximum achievable system Erlang capacity. Also, for a given value of the utilization factor of the primary channels, as the relative service time increases, the departure rate of successfully terminated calls decreases relative to the arrival rate of primary sessions; thus, the average number of idle channels decreases in detrimental of the new call blocking probability and, consequently, in detrimental of system capacity. The joint effect of these facts leads us to the behavior explained above and illustrated in Fig. 8.

Figure 9 plots the optimal number of reserved channels needed to maximize the system Erlang capacity. The maximum achieved Erlang capacity as function of the primary channel utilization factor for the scenarios described in Table 6 (both SH and NSH cases are considered) is shown in Fig. 8. Figure 9 confirms that as either mobility parameter or relative service time increases, more channels to prioritize intra- and inter-cell handoff call attempts over new call requests are reserved to guarantee the required QoS of secondary users.

On the other hand, for offered traffic loads given by the Erlang capacity values presented in Fig. 8, Fig. 10 plots, the inter-cell handoff arrival rate as a function of the utilization factor of the primary channels for the scenarios described in Table 6 (both SH and NSH cases are considered). Figure 10 presents both simulation (denoted by label "S") and analytical (denoted by label "A") results. Excellent agreement between analytical and simulation results is observed in Fig. 10. As expected, Fig. 10 shows that, for a given value of ρ and while system capacity is maximized, handoff arrival rate increases as the mobility parameter increases. For instance, let us consider the spectrum handoff scenarios with small relative service time (i.e., scenarios S1 and S3). Figure 10 shows that, for $\rho = 0.05$, the inter-cell handoff arrival rate increases 262% as the mobility parameter goes from 0.2 (scenario S1) to 1.0 (scenario S3). Figure 10 also shows that, for a given value of ρ and while system capacity is maximized, handoff arrival rate decreases as the relative service time increases. This behavior is due to the fact that as the relative service time increases, it is more likely that an ongoing secondary call to be interrupted due to the arrival of a primary session, consequently, a lower average number of ongoing calls are handed-off to adjacent cells (that is, the handoff rate decreases as the relative service time increases). Finally, Table 7 presents the maximum percentage difference of analytical results relative to simulation results for both new call blocking and forced call termination probabilities in order to achieve the Erlang capacity presented in Fig. 8. Two approaches for evaluating forced termination probability are considered in Table 7: the closed-form approximated expression (65) and the rate ratio approach represented by (66). Table 7 indicates that the maximum percentage difference between analytical and simulation results found for new call blocking probability is 1.4%. Similar results were found for the handoff rate, interruption probability, and inter-cellular handoff failure probability. On the other hand, Table 7 reveals that, for low mobility scenarios and irrespective of the relative service time (i.e., scenarios S1 and S2), the maximum percentage difference between analytical and simulation results found for the forced call termination probability is 2.4% {25%} if expression (66) {(65)} is used for evaluating this probability. In general, from Table 7, it can be concluded that expression (66) is the best option to evaluate forced call termination probability, except for the case when SH is used and scenario S3 is considered.

7 Conclusions

In this paper, teletraffic performance and channel holding time characterization in mobile cognitive radio cellular networks (CRCNs) under fixed-rate traffic with hard-delay constraints was investigated. To this end, a fundamental mathematical model to capture the effect of interruption of secondary users' calls due to the arrival of primary users was developed. Based on this model, closed-form mathematical expressions for the probability distribution function of channel holding time for new calls (CHTn) and handed-off calls (CHTh), call forced termination probability, and inter-cell handoff attempt rate were derived. Additionally, a teletraffic analysis for the performance evaluation of CRCNs in terms of the Erlang capacity was developed. The accuracy, applicability, and robustness of our proposed mathematical models were extensively investigated under a variety of different evaluation scenarios for all the considered call-level performance metrics. Although numerical results are extracted from particular scenarios with certain set of parameter values, our contribution clearly shows that there exist relevant sensitive issues

Table 7 Maximum relative difference between analytical and simulation numerical results for both forced call termination and new call blocking probabilities

Network type	Scenario	Forced call termination probability		New call blocking probability
		Using (67) (%)	Using (68) (%)	Using (63) (%)
With spectrum handoff (SH)	S1	15	2.4	0.7
	S2	25	0.8	0.4
	S3	7	12	1.4
	S4	15	4	1.0
Without spectrum handoff (NSH)	S1	1	0.5	0.8
	S3	1	0.5	1.3

concerning interruption time (IT), cell dwell time (CDT), unencumbered service time (UST), and certain parameters of the primary network (i.e., mean service time, channels usage) that significantly influence the performance of the secondary network. Numerical results reveal that the first three standardized moments of both CHTn and CHTh are highly sensitive to both interruption probability and type of probability distribution functions used to model CDT and UST. From the teletraffic point of view, numerical results demonstrate that system Erlang capacity strongly depends on the relative value of the mean secondary service time to the mean primary service time, users' mobility, whether or not spectrum handoff (SH) is used, and the primary channel utilization factor. Furthermore, numerical results reveal that there exists a critical utilization factor of the primary resources from which it is no longer possible to guarantee the required QoS of SUs and, therefore, delay sensitive services cannot be even supported in CRCNs. Thus, it is of paramount importance to develop mechanisms that effectively mitigate the adverse effects of service interruption of SUs in cognitive radio networks. Also, improvement of the accuracy of the forced call termination probability metric is a research topic of interest.

8 Endnotes

[1]For this type of traffic, it is considered that both blocked and interrupted (due to either inter-cell or intra-cell handoff failures) sessions are clear from the system. That is, a secondary type of traffic that has the most stringent QoS requirements (such as the unsolicited grant service class in mobile WiMAX) is considered.

[2]The accuracy of this proposed mathematical approach is extensively investigated under a variety of different evaluation scenarios for all the considered call-level performance metrics.

[3]System-level analysis involves statistics such as channel holding times for successful terminated calls and for forced terminated calls which are easily obtained at real networks while link-level statistics involve channel characterization (i.e., in terms of channel states characteristics and the probability distributions of the channel states duration), which are not easily obtained at real cellular networks.

[4]It is important to point out that in order to guarantee quality of service of secondary real-time traffic, in the literature, it has been proposed to reserve spectrum resources for exclusive use of the secondary users [13] but this is not considered in this manuscript.

[5]Considering Poisson arrivals for PUs, mathematical expressions for P_{Int} are derived in [36] and [37]. It is assumed that the UST for SUs is exponentially [36] and two-phase Coxian [37] distributed. For completeness, in Section 5, the mathematical expression of P_{Int} for exponentially distributed UST of SUs is shown.

[6]In general, the interruption probability is not independent. Indeed, when the traffic load is high, whenever a SU is interrupted due to the arrival of a PU, it is highly probable that the next arrival of a PU also causes the interruption of another secondary session because resource occupancy conditions at the different time instants (primary arrival epochs) are not independent. Conversely, in a low traffic load scenario, if the arrival of a PU does not cause an interruption of a SU, it is unlikely that the arrival of another PU in the same conditions causes a SU interruption. Hence, a certain degree of correlation between the interruption probabilities is present, and therefore, the secondary users' call interruption process actually is not a Poissonian one.

[7]The mathematical analysis for the phase-type probability distributions of both UST and CDT can be developed in a similar way, considering more state variables.

9 Appendix 1

In this Appendix, we show that the call interruption process is not a Poisson process. For this, the Bayes theorem is employed and we assume that the call interruption time due to arrival of PUs $X_{\text{int\_PU}}$ follows an

exponential distribution with parameter $\lambda^{(P)}P_{\text{Int}}$. Additionally, it is assumed that both the unencumbered service time and cell dwell time for SUs are exponentially distributed with parameters μ and η, respectively.

Notice that the call interruption time $X_{\text{int\_PU}}$ is not a measurable physical quantity because it is a potential time (when the interruption of a call does not occur, it is not possible to know its value), as explained in Section 2.1. Then, to show whether or not the call interruption process is Poissonian, we are interested on finding the probability distribution of a measurable physical quantity that can be obtained from our discrete-event computer simulator. In particular, we are interested on the conditional call interruption time given that calls are interrupted by the arrival of PUs which pdf is represented by $f_{X_{\text{int\_PU}}|X_{\text{int\_PU}}<\min(X_d,,X_s)}(t)$.

Let $X_c = \min(X_d, X_s)$ represent the channel holding time, then

$$f_{X_{\text{int\_PU}}|X_{\text{int\_PU}<X_c}}(t) = \frac{P\left(X_{\text{int\_PU}} < X_c \middle| X_{\text{int\_PU}} = t\right) f_{X_{\text{int\_PU}}}(t)}{P\left(X_{\text{int\_PU}} < X_c\right)} \tag{68}$$

From this, it is easy to say that

$$P\left(X_{\text{int\_PU}} < X_c \middle| X_{\text{int\_PU}} = t\right) = \int_t^{\infty} f_{X_c}(x)dx = e^{-(\eta+\mu)t} \tag{69}$$

On the other hand,

$$P\left(X_{\text{int\_PU}} < X_c\right) = \frac{\lambda^{(P)}P_{\text{Int}}}{\mu + \eta + \lambda^{(P)}P_{\text{Int}}} \tag{70}$$

Substituting (69) and (70) in (68), we get

$$f_{X_{\text{int}_{\text{PU}}}|X_{\text{int}_{\text{PU}}} < X_c}(t) = \left(\mu+\eta + \lambda^{(P)}P_{\text{Int}}\right)e^{-\left(\mu+\eta+\lambda^{(P)}P_{\text{Int}}\right)t} \tag{71}$$

Therefore, it has been shown that if the call interruption time due to arrival of PUs $X_{\text{int\_PU}}$ follows an exponential distribution, then the conditional call interruption time given that calls are interrupted by the arrival of PUs must be also exponentially distributed with mean

$$E\left\{X_{\text{int\_PU}} \middle| X_{\text{int\_PU}} < X_c\right\} = \frac{1}{\mu + \eta + \lambda^{(P)}P_{\text{Int}}} \tag{72}$$

and with coefficient of variation (CoV) equal to 1.

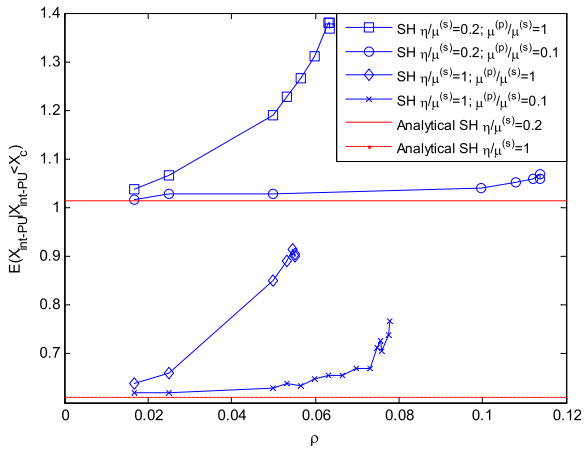

Fig. 11 Mean of the conditional call interruption time given that calls are interrupted by the arrival of PUs for different values of the primary channel utilization factor (ρ)

Again, this result is obtained assuming that the call interruption process is a Poisson process. Now, in Figs. 11 and 12, we compare, respectively, the mean and coefficient of variation of the conditional call interruption time given that calls are interrupted by the arrival of PUs obtained analytically (red symbols) and by simulation (blue lines) for the evaluation scenarios and conditions used in Section 5. From these numerical results, it is clear that the coefficient of variation differs from 1. Hence, the call interruption process is not actually a Poisson process.

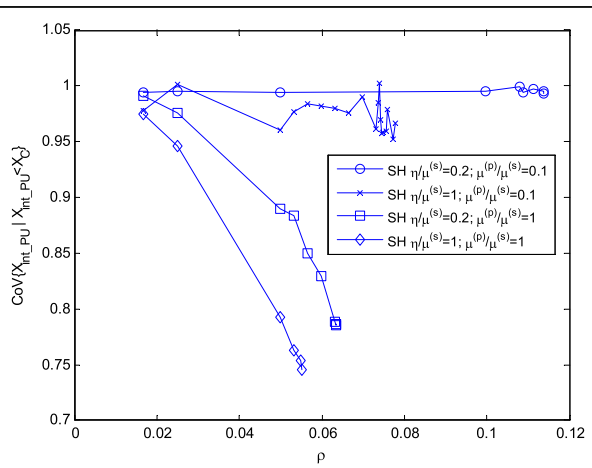

Fig. 12 Coefficient of variation of the conditional call interruption time given that calls are interrupted by the arrival of PUs for different values of the primary channel utilization factor (ρ)

10 Appendix 2

The Laplace Transform of the pdf of $X_{\text{Int\_PU}}$, given by (3), is calculated as

$$f^*_{X_{\text{int\_PU}}}(s) = \frac{\lambda^{(P)} P_{\text{Int}}}{\lambda^{(P)} P_{\text{Int}} + s} \tag{73}$$

It is clear that the unique pole of $f_{Xint\_PU}{}^*(-s)$ is $\Omega_{X_{\text{int\_PU}}} = \left\{\lambda^{(P)} P_{\text{Int}}\right\}$.

11 Appendix 3

In this Appendix, different statements used in the mathematical analysis are proven.

1. The statement $P\left\{X_{r,d} < \min\left(X_{\text{int\_PU}}, X_s\right)\right\} = f^*_{X_{r,d}}\left(\mu + \lambda^{(P)} P_{\text{Int}}\right)$ (where $X_{r,d}$ is either X_r or X_d) is proven as follows. Since X_{int_PU} and X_s are exponentially distributed, then the minimum between these variables is also exponentially distributed with parameter $\mu + \lambda^{(P)} P_{\text{Int}}$. As such,

$$f^*_{\min\left(X_{\text{int\_PU}}, X_s\right)}(s) = \frac{\mu + \lambda^{(P)} P_{\text{Int}}}{\mu + \lambda^{(P)} P_{\text{Int}} + s} \tag{74}$$

Using proposition 2 of [9],

$$P\left\{X_{r,d} < \min\left(X_{\text{int\_PU}}, X_s\right)\right\} = -\lim_{s \to \mu + \lambda^{(P)} P_{\text{Int}}} \frac{\left(s - \mu - \lambda^{(P)} P_{\text{Int}}\right) f^*_{X_{r,d}}(s)}{s} \cdot \frac{\mu + \lambda^{(P)} P_{\text{Int}}}{\mu + \lambda^{(P)} P_{\text{Int}} - s} \tag{75}$$

From this, it follows that

$$P\left\{X_{r,d} < \min\left(X_{\text{int\_PU}}, X_s\right)\right\} = f_{X_{r,d}}{}^*\left(\mu + \lambda^{(P)} P_{\text{Int}}\right) \tag{76}$$

2. The statement $P\left\{X_{\text{int\_PU}} < \min\left(X_{d,r}, X_s\right)\right\} = \frac{\lambda^{(P)} P_{\text{Int}}\left[1 - f^*_{X_{d,r}}\left(\mu + \lambda^{(P)} P_{\text{Int}}\right)\right]}{\mu + \lambda^{(P)} P_{\text{Int}}}$ (where $X_{d,r}$ is either X_d or X_r) is proven as follows. Let us define $Z_{d,r} = \min(X_{d,r}, X_s)$. Calculating the Laplace transform using proposition 2 of [9] we get

$$f^*_{Z_{d,r}}(s) = \frac{\mu}{\mu + s} + s\frac{f^*_{X_{d,r}}(\mu + s)}{\mu + s} = \frac{\mu + s f^*_{X_{d,r}}(\mu + s)}{\mu + s} \tag{77}$$

Since $P\{X_{\text{int\_PU}} < \min(X_{d,r}, X_s)\} = P\{X_{\text{int\_PU}} < Z_{d,r}\}$, using proposition 1 of [9], we obtain

$$P\left\{X_{\text{int\_PU}} < Z_{d,r}\right\} = \frac{\lambda^{(P)} P_{\text{Int}}\left[1 - f^*_{X_{d,r}}\left(\mu + \lambda^{(P)} P_{\text{Int}}\right)\right]}{\mu + \lambda^{(P)} P_{\text{Int}}} \tag{78}$$

3. Now, let us prove the statement $P\left\{X_d < \min\left(X_{\text{int\_PU}}, X_{sr}\right)\right\} = -\sum_{p \in \Omega_{X_d}} \mathbf{Res}_{s=p} \frac{\left[1 - f^*_{X_{sr}}\left(\lambda^{(P)} P_{\text{Int}} + s\right)\right] f^*_{X_d}(-s)}{\lambda^{(P)} P_{\text{Int}} + s}$.

To this end, the variable $\boldsymbol{Z}_{sr}$ is defined as follows $Z_{sr} = \min(X_{\text{int\_PU}}, X_{sr})$. The Laplace transform of the pdf of $\boldsymbol{Z}_{sr}$ is calculated using proposition 2 of [9] as

$$f^*_{Z_{sr}}(s) = \frac{\lambda^{(P)} P_{\text{Int}} + s f^*_{X_{sr}}\left(\lambda^{(P)} P_{\text{Int}} + s\right)}{\lambda^{(P)} P_{\text{Int}} + s} \tag{79}$$

Since $P\{X_d < \min(X_{\text{int\_PU}}, X_{sr})\} = P\{X_d < Z_{sr}\}$, using proposition 1 of [9], we obtain

$$P\{X_d < Z_{sr}\} = -\sum_{p \in \Omega_{X_d}} \mathbf{Res}_{s=p} \frac{\left[1 - f^*_{X_{sr}}\left(\lambda^{(P)} P_{\text{Int}} + s\right)\right] f^*_{X_d}(-s)}{\lambda^{(P)} P_{\text{Int}} + s} \tag{80}$$

4. Finally, in this section, the statement $P\left\{X_r < \min\left(X_{\text{int\_PU}}, X_s\right)\right\} = -\sum_{p \in \Omega_{X_r}} \mathbf{Res}_{s=p} \frac{\left[1 - f^*_{X_s}\left(\lambda^{(P)} P_{\text{Int}} + s\right)\right] f^*_{X_r}(-s)}{\lambda^{(P)} P_{\text{Int}} + s}$ is proven. To this end, the variable $\boldsymbol{Z}_s$ is defined as follows: $Z_s = \min(X_{\text{int\_PU}}, X_s)$. The Laplace transform of the pdf of $\boldsymbol{Z}_s$ is calculated using proposition 2 of [9] as

$$f^*_{Z_s}(s) = \frac{\lambda^{(P)} P_{\text{Int}} + s f^*_{X_s}\left(\lambda^{(P)} P_{\text{Int}} + s\right)}{\lambda^{(P)} P_{\text{Int}} + s} \tag{81}$$

Since $P\{X_r < \min(X_d, X_s)\} = P\{X_r < Z_s\}$, using proposition 1 of [9], we obtain

$$P\{X_r < Z_s\} = -\sum_{p \in \Omega_{X_r}} \mathbf{Res}_{s=p} \frac{\left[1 - f^*_{X_s}\left(\lambda^{(P)} P_{\text{Int}} + s\right)\right] f^*_{X_r}(-s)}{\lambda^{(P)} P_{\text{Int}} + s} \tag{82}$$

Acknowledgements
No one.

Funding
PRODEP contract 916040 and project no. 22411508 as well as UAM-A project no. EL001-13 provide us resources to acquire computing equipment for the numerical evaluation of the studied systems.

Authors' contributions
ALECR developed mathematical analysis for the channel holding times. He also obtained the numerical results obtained to evaluate the performance of the system in terms of the channel holding time. SLCL developed the teletraffic analysis and the optimization algorithm to maximize system Erlang capacity. She also participated in the mathematical analysis derived in this work and the numerical results obtained to evaluate the performance of the system. FACP was involved in the development of the different mathematical models as well as identifying, analyzing, and studying the

different factors that affect system performance. GHV was involved in the development of the different mathematical models as well as identifying, analyzing, and studying the different factors that affect system performance. MERA was involved in the mathematical analysis as well as in the numerical evaluation of the considered system. All authors read and approved the final manuscript.

Competing interests
The authors declare that they have no competing interests.

Publisher's Note

Author details
[1]Electrical Engineering Department, CINVESTAV-IPN, Mexico City, Mexico. [2]Electronics Department, UAM, Mexico City, Mexico. [3]Communication Networks Laboratory, CIC-Instituto Politécnico Nacional, Mexico City, Mexico.

Received: 21 April 2017 Accepted: 6 September 2017
Published online: 25 September 2017

References
1. X. Zhu, L. Shen, T.-S.P. Yum, Analysis of cognitive radio spectrum access with optimal channel reservation. IEEE Commun. Lett. **11**(4), 304–306 (2007)
2. Y.Y. Mihov, B.P. Tsankov, in *Proc. IEEE International Conference on Microwaves, Communications, Antennas and Electronics Systems (COMCAS 2011), Tel Aviv, Israel*. QoS provisioning via channel reservation in cognitive radio networks (2011)
3. S.L. Castellanos López, F.A. Cruz Pérez, M.E. Rivero-Ángeles, G. Hernández Valdez, in *Proc. 7th International Conference on Cognitive Radio Oriented Wireless Networks (CROWNCOM'2012), Stockholm, Sweden*. Impact of the primary resource occupancy information on the performance of cognitive radio networks with VoIP traffic (2012)
4. S.L. Castellanos-López, F.A. Cruz-Pérez, M.E. Rivero-Ángeles, G. Hernández-Valdez, Joint connection level and packet level analysis of cognitive radio networks with VoIP traffic. IEEE J. Select. Areas Commun. **32**(3), 601–614 (2014)
5. S.L. Castellanos-López, F.A. Cruz-Pérez, M.E. Rivero-Ángeles, G. Hernández-Valdez, Performance analysis of coordinated cognitive radio networks under fixed-rate traffic with hard delay constraints. J. Commun Netw Spec Issue Cogn Netw **16**(2), 130–139 (2014)
6. X. Mao, H. Ji, V.C.M. Leung, M. Li, in *Proc. IEEE GLOBECOM'2010, Miami, Florida, USA*. Performance enhancement for unlicensed users in coordinated cognitive radio networks via channel reservation (2010)
7. Y. Yao, S.R. Ngoga, D. Erman, A. Popescu, in *Proc. IEEE ICC'2012, Ottawa, Canada*. Performance of cognitive radio spectrum access with intra- and inter-handoff (2012), pp. 1549–1554
8. A.L.E. Corral-Ruiz, F.A. Cruz-Pérez, G. Hernández-Valdez, in *Proc. IEEE WCNC'2011, Cancun, QR, Mexico*. Channel holding time in mobile cellular networks with heavy-tailed distributed cell dwell time (2011), pp. 2065–2070
9. C.B. Rodríguez-Estrello, G. Hernández-Valdez, F.A. Cruz-Pérez, System-level analysis of mobile cellular networks considering link unreliability. IEEE Trans. Veh. Technol. **58**(2), 926–940 (2009)
10. X. Wang, P. Fan, Channel holding time in wireless cellular communications with general distributed session time and dwell time. IEEE Commun. Lett. **11**(2), 158–160 (2007)
11. P.V. Orlik, S.S. Rappaport, A model for teletraffic performance and channel holding time characterization in wireless cellular communication with general session and dwell time distributions. IEEE J. Sel. Areas Commun. **16**(5), 788–803 (1998)
12. A.L.E. Corral-Ruiz, F.A. Cruz-Pérez, G. Hernández-Valdez, in *Proc. IEEE GLOBECOM'2010, Miami, Florida*. On the functional relationship between channel holding time and cell dwell time in mobile cellular networks (2010)
13. D. Cavdar, H.B. Yilmaz, T. Tugcu, F. Alagöz, in *Proc. 6th Advanced International Conference on Telecommunications (AICT'2010), Barcelona, Spain*. Analytical modeling and performance evaluation of cognitive radio networks (2010), pp. 35–40
14. W.-Y. Lee, I.F. Akyildiz, Spectrum-aware mobility management in cognitive radio cellular networks. IEEE Trans. Mob. Comput. **11**(4), 529–542 (2012)
15. Y. Fang, I. Chlamtac, Y.B. Lin, Channel occupancy times and handoff rate for mobile computing and PCS networks. IEEE Trans. Comput. **47**(6), 679–692 (1998)
16. Y. Fang, I. Chlamtac, Teletraffic analysis and mobility modeling of PCS networks. IEEE Trans. Commun. **47**(7), 1062–1072 (1999)
17. Y. Zhang, B. Soong, Performance of mobile network with wireless channel unreliability and resource insufficiency. IEEE Trans. Wirel. Commun. **5**(5), 990–995 (2006)
18. Y. Zhang, M. Fujise, Performance analysis of wireless networks over Rayleigh fading channel. IEEE Trans. Veh. Technol. **55**(5), 1621–1632 (2006)
19. Y. Zhang, M. Ma, M. Fujise, Call completion in wireless networks over lossy link. IEEE Trans. Veh. Technol. **56**(2), 929–942 (2007)
20. Y. Yao, A. Popescu, A. Popescu, On prioritised opportunistic spectrum access in cognitive radio cellular networks. Trans. Emerg. Telecommun. Technol. **27**(2), 294–310 (2016)
21. A. Homayounzadeh, M. Mahdavi, *Quality of Service Analysis for the Real-Time Secondary Users in Cognitive Radio Cellular Networks, Accepted for Its Publication in Wireless Personal Communications, First Online* (2017). https://doi.org/10.1007/s11277-017-4340-y
22. Hau-luen Chiou, "Performance Evaluation of Multirate Cognitive Radio Cellular Networks with Channel Aggregation", Master's Thesis, Department of Electrical Engineering, Date of Defense: 2014
23. J. Serrano-Chavez, G. Hernandez-Valdez, F.A. Cruz-Pérez, S.L. Castellanos-Lopez, E.A. Andrade-Gonzalez, M. Reyes-Ayala, J.R. Miranda-Tello, in *Proc. WSEAS Recent Advances on Systems, Signals, Control, Communications and Computers (DNCOCO'15), Budapest, Hungary*. Impact of mobility on the performance of cognitive radio mobile cellular networks with real-time traffic (2015), pp. 236–242
24. D. Cavdar, H.B. Yilmaz, T. Tugcu, F. Alagöz, Analytical modeling and resource planning for cognitive radio systems. Wirel. Commun. Mob. Comput. **12**(3), 277–292 (2012)
25. Y. Fang, Performance evaluation of wireless cellular networks under more realistic assumptions. Wirel. Commun. Mob. Comput. **5**(8), 867–885 (2005)
26. Y. Fang, Modeling and performance analysis for wireless mobile networks: A new analytical approach. IEEE/ACM Trans. Networking **13**(5), 989–902 (2005)
27. S. Tang, B.L. Mark, Modeling and analysis of opportunistic spectrum sharing with unreliable spectrum sensing. IEEE Trans. Wirel. Commun. **8**(4), 1934–1943 (2009)
28. I. Suliman, J. LehtomLki, T. BrLysy, K. Umebayashi, in *Proc. IEEE PIMRC'2009, Tokyo, Japan*. Analysis of cognitive radio networks with imperfect sensing (2009), pp. 1616–1620
29. X. Gelabert, O. Salient, J. Prez-Romero, R. Agust, Spectrum sharing in cognitive radio networks with imperfect sensing: A discrete-time Markov model. Comput. Netw. **54**(14), 2519–2536 (2010)
30. S. Tang, A general model of opportunistic spectrum sharing with unreliable sensing. Int. J. Commun. Syst. **27**(1), 31–34 (2014)
31. J. Martinez-Bauset, V. Pla, J.R. Vidal, L. Guijarro, Approximated analysis of cognitive radio systems using time-scale separation and its accuracy. IEEE Commun. Lett. **17**(1), 35–38 (2013)
32. O. Salameh, K. de Turck, D. Fiems, H. Bruneel, and S. Wittevrongel, "Performance Analysis of a Cognitive Radio Network with Imperfect Spectrum Sensing," IEICE Trans. on Communications, Advance Publication: Released June 22, 2017. https://doi.org/10.1587/transcom.2017EBP3037
33. J.-W. Wang, R. Adriman, in *Proc. (IMIS'2013), Taichung, Taiwan*. Analysis of cognitive radio networks with imperfect sensing and backup channels (2013), pp. 626–631
34. F. Wang, J. Huang, Y. Zhao, Delay sensitive communications over cognitive radio networks. IEEE Trans. Wirel. Commun. **11**(4), 1402–1411 (2012)
35. L. Duan, J. Huang, B. Shou, Investment and pricing with spectrum uncertainty: A cognitive operator's perspective. IEEE Trans. Mob. Comput. **10**(11), 1590–1604 (2011)
36. Y. Zhang, in *Proc. IEEE ICC'2008, Beijing, China*. Dynamic spectrum access in cognitive radio wireless networks (2009), pp. 4927–4932
37. S.L. Castellanos-Lopez, F.A. Cruz-Perez, G. Hernandez-Valdez, in *Proc. 7th IEEE International Conference on Wireless and Mobile Computing, Networking and Communications (WiMob'2011), Shangai, China*. Performance of cognitive radio networks under resume and restart retransmission strategies (2011), pp. 51–59
38. F.A. Cruz-Pérez, D. Lara-Rodríguez, M. Lara, Fractional channel reservation in mobile communication systems. IEE Electron. Lett. **35**(23), 2000–2002 (1999)
39. R. Ramjee, R. Nagarajan, D. Towsley, On optimal call admission control in cellular networks. ACM/Baltzer Wirel. Netw. J. **3**(1), 29–41 (1997)

40. D. Sarkar, T. Jewell, S. Ramakrishnan, Convergence in the calculation of the handoff arrival rate: A log-time iterative algorithm. EURASIP J. Wirel. Commun. Netw. **2006**(1), 1–11 (2006)
41. M. Zhang, C.T. Lea, On the mobility/capacity conversion in wireless networks. IEEE Trans. Veh. Technol. **53**(3), 734–746 (2004)